Received March 12, 2019, accepted March 22, 2019, date of publication April 2, 2019, date of current version April 17, 2019.

Digital Object Identifier 10.1109/ACCESS.2019.2908882

Spectral- and Energy-Efficiency of Multi-Pair Two-Way Massive MIMO Relay Systems Experiencing Channel Aging

LIXIN LI [1], (Member, IEEE), JIAO HE [2], LIE-LIANG YANG [3], (Fellow, IEEE), ZHU HAN [4,5], (Fellow, IEEE), MIAO PAN [4], (Senior Member, IEEE), WEI CHEN [6], (Senior Member, IEEE), HUISHENG ZHANG [1], AND XU LI [1]

[1] School of Electronics and Information, Northwestern Polytechnical University, Xi'an 710072, China
[2] Xi'an ASN Technology Group Co., Ltd., Xi'an 710072, China
[3] School of Electronics and Computer Science, The University of Southampton, Southampton SO17 1BJ, U.K.
[4] Department of Electrical and Computer Engineering, University of Houston, Houston, TX 77004, USA
[5] Department of Computer Science and Engineering, Kyung Hee University, Seoul 446-701, South Korea
[6] Department of Electronics Engineering, Tsinghua University, Beijing 100084, China

Corresponding author: Lixin Li (lilixin@nwpu.edu.cn)

This work was supported in part by the Aerospace Science and Technology Innovation Fund of the China Aerospace Science and Technology Corporation, in part by the Shanghai Aerospace Science and Technology Innovation Fund under Grant SAST2018045, Grant SAST2016034, and Grant SAST2017049, in part by the EPSRC under Project EP/P034284/1 and the Innovate U.K. Project, in part by the U.S. MURI AFOSR under Grant MURI 18RT0073, Grant NSF CNS-1717454, Grant CNS-1731424, Grant CNS-1702850, Grant CNS-1646607, Grant CNS-1350230, Grant CNS-1646607, and Grant CNS-1801925, in part by the National Natural Science Foundation of China under Grant 61671269, and in part by the Beijing Natural Science Foundation under Grant 4191001.

ABSTRACT In this paper, we demonstrate the impact of channel aging on the spectral- and energy-efficiency performance of the multi-pair two-way massive MIMO relay (MTW-MMR) systems, where massive antennas are deployed at the relay and the amplify-and-forward (AF) protocol is operated. By assuming the maximum-ratio combining/maximum-ratio transmission (MRC/MRT) or zero-forcing reception/zero-forcing transmission (ZFR/ZFT) relaying processing, we analyze the spectral efficiency (SE) and energy efficiency (EE) of the MTW-MMR systems experiencing both imperfect channel estimation and channel aging based on the four proposed power-scaling schemes. Furthermore, we compare the performance of the full-duplex (FD)-assisted MTW-MMR systems with that of the half-duplex (HD)-assisted MTW-MMR systems, showing that the FD mode outperforms the HD mode with the interference level not exceeding −15 dB. Our studies show that channel aging may significantly degrade the achievable performance in terms of SE and EE. However, the inter-pair interference caused by the other user pairs and the self-interference can be effectively mitigated by the MRC/MRT processing or ZFR/ZFT processing at the relay.

INDEX TERMS Massive MIMO, two-way relay, full-duplex, half-duplex, channel aging, maximum-ratio combining/maximum-ratio transmission, zero-forcing reception/zero-forcing transmission, spectral-efficiency, energy-efficiency.

I. INTRODUCTION

The 5th generation (5G) mobile communication systems [2] demand higher spectral-efficiency (SE) and higher energy-efficiency (EE) [3], [4]. In order to achieve these objectives, massive multiple-input multiple-output (MIMO) [5], cooperative communications [6], and full-duplex (FD) [7]–[9] have been drawn a lot of attention. According to literature [5], massive MIMO is capable of effectively enhancing the SE and EE via providing a large array gain and a spatial multiplexing gain. By contrast, cooperative relaying is capable of extending coverage and increasing diversity gain without consuming extra power. Among the various cooperative relaying schemes, the two-way relaying allows

The associate editor coordinating the review of this manuscript and approving it for publication was Shuai Han.

two users to exchange their information with the aid of a relay, and hence has been recognized as an efficient scheme for achieving high SE in contrast to the traditional one-way relaying [10]. Furthermore, the concept of massive MIMO has been introduced to the two-way relay systems in order to further improve their SE and EE [11]. On the other side, owing to the capability to simultaneously transmit and receive on the same frequency, FD technologies can significantly enhance the systems SE in comparison to the conventional half-duplex (HD) technologies [12], besides, the two-path successive relay system [13] mimicking an FD relay system can also improve the system SE.

The interference cancellation and the interference mitigation have been widely studied in 5G communication systems [14], [15]. Recently, massive MIMO has been introduced to the FD-assisted two-way relay systems in order to suppress the loop interference in the spatial domain [16]. The authors in [17], [18] proposed a multi-pair two-way massive MIMO relay (MTW-MMR) system operated in the FD mode, and studied its performance under perfect channel state information (CSI) and when employing maximum-ratio combining/maximum-ratio transmission (MRC/MRT) relay processing. However, assuming the perfect CSI is unrealistic. Thus, the authors in [19] concentrated on the FD-assisted MTW-MMR systems with imperfect CSI, when the zero-forcing reception/zero-forcing transmission (ZFR/ZFT) relay processing is employed. In literature [20], the sum rate of the FD-assisted MTW-MMR systems with MRC/MRT relay processing was considered, and in [21], the asymptotic sum-rate the authors of the FD-assisted TW-MMR systems with ZFR/ZFT relay processing considering the impact of antenna correlation was studied. While in [22], the SE and EE performance of the FD-assisted MTW-MMR systems were studied when assuming imperfect CSI and considering several power scale schemes. By assuming perfect CSI or imperfect CSI, the SE and EE of the FD-assisted MTW-MMR systems were investigated and compared when MRC/MRT and ZFR/ZFT relay processing schemes were considered [23].

When assuming the HD mode, the authors in [24] investigated the ergodic rate of a massive MIMO supported two-way relay network with perfect CSI. In the case of imperfect CSI, the authors in [25], [26] studied the SE and EE performance of a MTW-MMR system operated in the HD mode with MRC/MRT relay processing. Furthermore, the impact of co-channel interference (CCI) and pilot contamination were considered in [27] to investigate the achievable performance of the MTW-MMR system operated in the HD mode. Later, the authors in [28] presented a FD-assisted massive MIMO two-way relay cellular network, and compared its achievable performance with the HD relaying mode. Similarly, in [29], the performance of the FD-assisted TW-MMR system with MRC/MRT relay processing operated under either the FD mode or the HD mode was studied and compared, when four power-scaling cases were considered. Moreover, in [30]–[34], the SE and EE of both the FD-assisted and HD-assisted MTW-MMR systems were respectively investigated and compared, when assuming imperfect CSI, and MRC/MRT or ZFR/ZFT relay processing, and when communicating over the Ricean fading channels. Besides, the authors in [35]–[38] studied the power-allocation problem in order to maximize the system performance of the TW-MMR systems.

In addition to CSI, channel aging is another factor having a big impact on the achievable performance of wireless communication systems. Channel aging represents the phenomenon causing the mismatch between the channels applied for precoding/detection and the real channels due to delay. Channel aging was studied in the context of massive MIMO systems operated in different scenarios [39]–[45]. Specifically for relay communications, the authors in [46] investigated the SE of the multi-pair massive MIMO relay networks with the MRC/MRT relay processing, when channel aging effect is considered. By contrast, the sum-rate of a single-pair FD-assisted TW-MMR system with the MRC/MRT relay processing was studied in [47] by taking the channel aging into account.

From literature, we can observe that the FD-assisted MTW-MMR system with both perfect and imperfect CSI has been well studied. However, the channel aging effect has not been sufficiently analyzed in the context of the MTW-MMR systems operated in the FD mode. Note that multi-pair systems are more general and complex than single-pair systems, as there are more types of interference in multi-pair FD systems, including inter-pair interference, inter-user interference and self-loop interference, which can result in the losses of SE and EE.

In this paper, we investigate the SE and EE of the MTW-MMR systems, when jointly considering the imperfect CSI and channel aging effect. Both FD mode and HD mode are considered to characterize the system performance. When the MRC/MRT or ZFR/ZFT relay processing is employed, the asymptotic SE and EE of the FD-assisted and HD-assisted MTW-MMR systems are derived under the proposed four power scaling schemes. With the aid of numerical and simulation results, we compare the SE and EE between the FD-assisted and HD-assisted MTW-MMR systems, showing that the FD scheme outperforms the HD scheme. Moreover, our studies show that both the inter-pair interference and self-interference can be effectively eliminated by the MRC/MRT processing or ZFR/ZFT processing operated at the relay. However, the channel aging usually leads to the reduction of SE and EE. Our main contributions in this paper can be summarized as follows:

- To the best of our knowledge, we are the first to jointly consider the imperfect CSI and channel aging in the context of the MTW-MMR systems.
- With the transmit power of the users or the transmit power of the relay remaining constant or scaling down to $1/N$, respectively, we propose four power scaling schemes. Under these power scaling schemes, the asymptotic SE and EE of the FD-assisted and

HD-assisted MTW-MMR systems with MRC/MRT or ZFR/ZFT relay processing are derived.

- The SE and EE of the FD-assisted MTW-MMR systems and that of the HD-assisted MTW-MMR systems are investigated and compared based on theoretical analysis and simulations.

The rest of the paper is organized as follows. Section II describes the system model. In Section III, we analyze the asymptotic SE and EE of the FD-assisted and HD-assisted MTW-MMR systems, when different operational scenarios are considered. Simulation results are provided in Section IV, and finally we draw the conclusions from research in Section V.

Notations: Boldface uppercase and boldface lowercase variables represent matrices and column vectors, respectively. $(\cdot)^T$, $(\cdot)^H$, $(\cdot)^*$, $(\cdot)^{-1}$, $\mathrm{Tr}(\cdot)$, $\|\cdot\|$, and $\mathbb{E}\{\cdot\}$ stand for the transpose, conjugate transpose, conjugate, inverse of a matrix, trace of a square matrix, Euclidean norm and the expectation, respectively. $\mathcal{CN}\left(\mu, \sigma^2\right)$ denotes a complex Gaussian distribution with a mean of μ and a variance of σ^2. $\boldsymbol{I}_N$ denotes an $(N \times N)$ identity matrix.

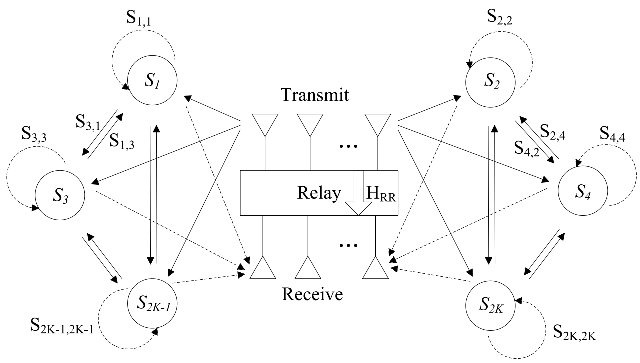

FIGURE 1. Schematic diagram for the multi-pair massive MIMO two-way relay system employing full-duplex AF protocol.

II. SYSTEM MODEL

Consider a MTW-MMR system with the amplify-forward (AF) protocol. As shown in Fig. 1, there are K pairs of user nodes, and the mth pair of (S_{2m-1}, S_{2m}) $(m = 1, \cdots, K)$ communicate with each other via a relay node equipping with a massive number of antennas. We assume that the users in $\{S_{2K-1}\}$ and those in $\{S_{2K}\}$ are sufficiently separated, making the interference between them ignorable. Furthermore, we assume a flat-fading channel model, and that the channel coefficients remain constant within one symbol duration, and change slowly from one symbol to another.

A. SIGNAL TRANSMISSION

In the considered system of Fig. 1, all nodes are assumed to be operated in the FD mode, and each user is equipped with two antennas, in which one is for signal transmission and the other one is for receiving. By contrast, the relay node has N transmit antennas and N receive antennas.

At time instant n, S_k, $k = 1, 2, \cdots 2K$, transmits the signal of $\sqrt{P_S}x_k(n)$ to the relay node, and the relay node broadcasts the signal $\boldsymbol{x}_R(n) \in \mathbb{C}^{N\times 1}$ to all the $2K$ users. We assume that all users experience the same average power constraint of P_S and hence, we have $\mathbb{E}\left\{|x_k(n)|^2\right\} = 1$. The power constraint on the relay is denoted by P_R, which is experienced as $\mathrm{Tr}\left(\mathbb{E}\left\{\boldsymbol{x}_R(n)\boldsymbol{x}_R^H(n)\right\}\right) \le P_R$. Based on the above assumptions, the received signals at the relay and at user k can be written as

$$\begin{aligned} \boldsymbol{y}_R^{FD}(n) &= \sum_{k=1}^{2K} \boldsymbol{h}_{uk}\sqrt{P_S}x_k(n) + \boldsymbol{H}_{RR}\boldsymbol{x}_R(n) + \boldsymbol{z}_R(n) \\ &= \sqrt{P_S}\boldsymbol{H}_u\boldsymbol{x}(n) + \boldsymbol{H}_{RR}\boldsymbol{x}_R(n) + \boldsymbol{z}_R(n), \end{aligned} \tag{1}$$

$$y_k^{FD}(n) = \boldsymbol{h}_{dk}^T\boldsymbol{x}_R(n) + \sum_{i,k\in\mathcal{U}_k} S_{k,i}\sqrt{P_S}x_i(n) + z_k(n), \tag{2}$$

where the superscript 'FD' is for 'full-duplex'. In (1) and (2) we define the set $\mathcal{U}_k = \{1, 3, \cdots, 2K-1\}$ or $\mathcal{U}_k = \{2, 4, \cdots, 2K\}$, determined by the index k in (2), $\boldsymbol{x}(n) = [x_1(n), x_2(n), \cdots, x_{2K}(n)]^T$. Furthermore, in (1), we define $\boldsymbol{H}_u = [\boldsymbol{h}_{u1}, \boldsymbol{h}_{u2}, \cdots, \boldsymbol{h}_{u2K}]$, where $\boldsymbol{h}_{uk} \in \mathbb{C}^{N\times 1}$ denotes the channels from the transmit antenna of S_k to the receive antenna array at the relay. Similarly, we define $\boldsymbol{H}_d = [\boldsymbol{h}_{d1}, \boldsymbol{h}_{d2}, \cdots, \boldsymbol{h}_{d2K}]$ for (2), where $\boldsymbol{h}_{dk}^T \in \mathbb{C}^{1\times N}$ contains the channels from the transmit antenna array of the relay to the receive antenna of S_k. We assume that $\boldsymbol{H}_u$ and $\boldsymbol{H}_d$ can be expressed as $\boldsymbol{H}_u = \boldsymbol{F}_u\boldsymbol{G}_u^{1/2}$ and $\boldsymbol{H}_d = \boldsymbol{F}_d\boldsymbol{G}_d^{1/2}$, respectively, where $\boldsymbol{F}_u$ and $\boldsymbol{F}_d$ stand for the small-scale fading with their elements being i.i.d. random variables obeying the distribution of $\mathcal{CN}(0, 1)$, while $\boldsymbol{G}_u$ and $\boldsymbol{G}_d$ are diagonal matrices taking into account of the large-scale fading, with the kth diagonal elements of $\boldsymbol{G}_u$ and $\boldsymbol{G}_d$ denoted as σ_{uk}^2 and σ_{dk}^2, respectively. In (1), $\boldsymbol{H}_{RR} \in \mathbb{C}^{N\times N}$ yields the self-loop interference at the relay, the elements of $\boldsymbol{H}_{RR}$ are random variables obeying the i.i.d. $\mathcal{CN}\left(0, \sigma_{RR}^2\right)$. By contrast, in (2), $S_{k,i}$ obeying the i.i.d. $\mathcal{CN}\left(0, \sigma_{k,i}^2\right)$ represents the inter-user interference, when $i, k \in \mathcal{U}_k, i \neq k$ and the self-loop interference, when $i = k$, on the S_k. Finally, in (1) and (2), $\boldsymbol{z}_R(n) \in \mathbb{C}^{N\times 1}$ and $z_k(n)$ are additive white Gaussian noise (AWGN) at the relay and at S_k, the elements of which obey the distributions of $\mathcal{CN}\left(0, \sigma_{nr}^2\right)$ and of $\mathcal{CN}\left(0, \sigma_n^2\right)$, respectively.

During the nth symbol period, the relay amplifies the signal $\boldsymbol{y}_R^{FD}(n-1)$ received during the $(n-1)$th symbol period, and broadcasts it to the $2K$ users. Thus, we have

$$\boldsymbol{x}_R(n) = \boldsymbol{W}_R(n)\boldsymbol{y}_R^{FD}(n-1) = \alpha(n)\boldsymbol{W}(n)\boldsymbol{y}_R^{FD}(n-1), \tag{3}$$

where $\boldsymbol{W}_R(n)$ is the amplification matrix, $\alpha(n)$ is the amplification factor, and $\boldsymbol{W}(n)$ is the processing matrix used by the relay for preprocessing. Thus, we have $\boldsymbol{W}_R(n) = \alpha(n)\boldsymbol{W}(n)$.

Upon substituting (1) and (3) into (2), the received signal at S_k is given by

$$\begin{aligned} y_k^{FD} &= \alpha\boldsymbol{h}_{dk}^T\boldsymbol{W}\boldsymbol{h}_{uk'}\sqrt{P_S}x_{k'} + \alpha\boldsymbol{h}_{dk}^T\boldsymbol{W}\boldsymbol{h}_{uk}\sqrt{P_S}x_k \\ &\quad + \alpha\boldsymbol{h}_{dk}^T\boldsymbol{W}\sum_{\substack{j=1\\ j\neq k,k'}}^{2K} \boldsymbol{h}_{uj}\sqrt{P_S}x_j + \sum_{i,k\in\mathcal{U}_k} S_{k,i}\sqrt{P_S}x_i \\ &\quad + \alpha\boldsymbol{h}_{dk}^T\boldsymbol{W}\boldsymbol{H}_{RR}\boldsymbol{x}_R + \alpha\boldsymbol{h}_{dk}^T\boldsymbol{W}\boldsymbol{z}_R + z_k, \end{aligned} \tag{4}$$

where the index $(n-1)$ and n are omitted for convenience of presentation. In detail, in (4), the first term is the desired signal sent from user k' to user k, here, $k'=2m$ or $k'=2m-1$, $k=2m-1$ or $k=2m$, when assuming that there is a user pair $(S_k, S_{k'})$, the second term is the self-interference reflected by the user k. After some necessary self-interference cancellation in the propagation and analog domains [48], the second term can be effectively eliminated. The third term is the inter-pair interference caused by the other $(K-1)$ user pairs. The fourth term consists of the self-loop interference and the inter-user interference as seen in (2). The fifth and sixth terms are the self-loop interference and noise received from the relay, respectively. And finally, the last term is the AWGN added at S_k.

When substituting (1) into (3) and applying the power constraint of $\mathrm{Tr}\left(\mathbb{E}\left\{\boldsymbol{x}_R(n)\boldsymbol{x}_R^H(n)\right\}\right) \le P_R$ on the relay, we obtain

$$\alpha(n) = \sqrt{\frac{P_R}{P_S \cdot \Delta_1(n) + \sigma_{nr}^2 \cdot \Delta_2(n) + \Delta_3(n)}}, \tag{5}$$

where $\Delta_1(n)$, $\Delta_2(n)$ and $\Delta_3(n)$ are, respectively, defined as

$$\Delta_1(n) = \mathrm{Tr}\left(\boldsymbol{W}(n)\boldsymbol{H}_u(n-1)\boldsymbol{H}_u^H(n-1)\boldsymbol{W}(n)^H\right), \tag{6}$$

$$\Delta_2(n) = \mathrm{Tr}\left(\boldsymbol{W}(n)\boldsymbol{W}(n)^H\right), \tag{7}$$

$$\Delta_3(n) = P_R\mathrm{Tr}\left[\left(\boldsymbol{W}(n)\boldsymbol{H}_{RR}\boldsymbol{H}_{RR}^H\boldsymbol{W}(n)^H\right)\right]. \tag{8}$$

In contrast to the FD systems, the HD systems don't suffer from the self-loop interference and the inter-user interference, as that described in the context of (4). Thus, with all the nodes operated in the HD mode, the received signals at the relay and at user k can be given, respectively, as

$$\begin{aligned} \boldsymbol{y}_R^{HD}(n) &= \sum_{k=1}^{2K}\boldsymbol{h}_{uk}\sqrt{P_S}x_k(n) + \boldsymbol{z}_R(n) \\ &= \sqrt{P_S}\boldsymbol{H}_u\boldsymbol{x}(n) + \boldsymbol{z}_R(n), \end{aligned} \tag{9}$$

$$y_k^{HD}(n) = \boldsymbol{h}_{dk}^T\boldsymbol{x}_R(n) + z_k(n), \tag{10}$$

where the superscript 'HD' is for 'half-duplex'. Furthermore, in (10)

$$\boldsymbol{x}_R(n) = \alpha(n)\boldsymbol{W}(n)\boldsymbol{y}_R^{HD}(n-1). \tag{10a}$$

Similarly to (4), after omitting the indices $(n-1)$ and n, the received signal at S_k can be written as

$$\begin{aligned} y_k^{HD} &= \alpha\boldsymbol{h}_{dk}^T\boldsymbol{W}\boldsymbol{h}_{uk'}\sqrt{P_S}x_{k'} + \alpha\boldsymbol{h}_{dk}^T\boldsymbol{W}\boldsymbol{h}_{uk}\sqrt{P_S}x_k \\ &\quad + \alpha\boldsymbol{h}_{dk}^T\boldsymbol{W}\sum_{\substack{j=1\\ j\neq k,k'}}^{2K}\boldsymbol{h}_{uj}\sqrt{P_S}x_j + \alpha\boldsymbol{h}_{dk}^T\boldsymbol{W}\boldsymbol{z}_R + z_k. \end{aligned} \tag{11}$$

Accordingly, applying the relay power constraint, $\alpha(n)$ in (10a) is given by

$$\alpha(n) = \sqrt{\frac{P_R}{P_S \cdot \Delta_1(n) + \sigma_{nr}^2 \cdot \Delta_2(n)}}, \tag{12}$$

associated with the definition

$$\Delta_1(n) = \mathrm{Tr}\left(\boldsymbol{W}(n)\boldsymbol{H}_u(n-1)\boldsymbol{H}_u^H(n-1)\boldsymbol{W}(n)^H\right), \tag{13}$$

$$\Delta_2(n) = \mathrm{Tr}\left(\boldsymbol{W}(n)\boldsymbol{W}(n)^H\right). \tag{14}$$

In comparison with (4), we observe that the self-loop interference and inter-user interference do not exist in (11) in the HD mode, but at the cost of halving the data rate at the extreme case.

B. CHANNEL ESTIMATION

Having provided the signal models, let us now consider the channel estimation issue. In FD mode, signals are transmitted simultaneously on both uplink users-to-relay and downlink relay-to-users channels, which interfere with each other, resulting in the challenges on channel estimation. In our study, we do not assume the reciprocity between the up and down links, but assume that the uplink and downlink channels are estimated separately, in order to obtain more accurate CSI.

In detail, we assume that CSI is estimated at the time instant 0. Specifically, the relay estimates the uplink channels using the uplink pilots sent by the $2K$ users. We assume that the length of pilot sequences is τ_u, and that the pilot matrix for uplink channel estimation is expressed as $\boldsymbol{X}^u \in \mathbb{C}^{2K\times\tau_u}$, which satisfies $\boldsymbol{X}^u(\boldsymbol{X}^u)^H = \boldsymbol{I}_{2K}$. Then, the signals received at the relay for channel estimation can be expressed as [39]

$$\boldsymbol{Y}^u(0) = \sqrt{\tau_u P_S}\boldsymbol{H}_u(0)\boldsymbol{X}^u + \boldsymbol{Z}_u(0), \tag{15}$$

where $\boldsymbol{Z}_u \in \mathbb{C}^{N\times\tau_u}$ is the AWGN obeying the i.i.d. $\mathcal{CN}(0,1)$, P_S is the power received from the pilots, while $\boldsymbol{H}_u(0)$ are the channels to be estimated.

Assuming the minimum-mean-square-error (MMSE) channel estimation [49], the estimate to $\boldsymbol{H}_u(0)$ is then given by

$$\begin{aligned} \tilde{\boldsymbol{H}}_u(0) &= \left(\boldsymbol{H}_u(0) + \frac{1}{\sqrt{\tau_u P_S}}\boldsymbol{Z}_u(0)\left(\boldsymbol{X}^u\right)^H\right) \\ &\quad \times \left(\frac{1}{\tau_u P_S}\boldsymbol{G}_u^{-1} + \boldsymbol{I}_{2K}\right)^{-1}, \end{aligned} \tag{16}$$

where $\boldsymbol{I}_{2K}$ is a $(2K\times 2K)$ identity matrix. Note that specifically, $\boldsymbol{h}_{uk}(0)$ can be expressed as

$$\boldsymbol{h}_{uk}(0) = \tilde{\boldsymbol{h}}_{uk}(0) + \Delta\boldsymbol{h}_{uk}(0), \tag{17}$$

where it can be shown that each element of $\tilde{\boldsymbol{h}}_{uk}(0)$ is a complex Gaussian random variable distributed with zero mean and a variance of $\hat{\sigma}_{uk}^2 = \frac{\tau_u P_S \sigma_{uk}^4}{1+\tau_u P_S \sigma_{uk}^2}$, $\Delta\boldsymbol{h}_{uk}(0)$ is the estimation error yielded by the MMSE estimator, which is independent of $\tilde{\boldsymbol{h}}_{uk}(0)$ owing to the properties of MMSE estimation.

Similarly, the downlink channel vector $\boldsymbol{h}_{dk}(0)$ can be estimated with the aid of the pilots sent by the relay, given as

$$\boldsymbol{h}_{dk}(0) = \tilde{\boldsymbol{h}}_{dk}(0) + \Delta\boldsymbol{h}_{dk}(0), \tag{18}$$

where $\tilde{\boldsymbol{h}}_{dk}(0)$ and $\Delta\boldsymbol{h}_{dk}(0)$ have the same explanation as the corresponding terms in (17). For the following analysis, we denote the variance of the elements in $\tilde{\boldsymbol{h}}_{dk}(0)$ as $\hat{\sigma}_{dk}^2$.

C. CHANNEL AGING

In our study, we also consider the impact of channel aging by introducing the model proposed in [39]. In this model, at time instant $(n+1)$, the uplink channel vector from the kth user to the relay can be expressed as

$$\boldsymbol{h}_{uk}[n+1] = \rho \boldsymbol{h}_{uk}[n] + \Delta \boldsymbol{e}_{uk}[n+1], \tag{19}$$

where $\rho = J_0(2\pi f_D T_S)$ is the temporal correlation parameter of the uplink channel, in which $J_0(\cdot)$ is the zeroth-order Bessel function of the first kind, T_S is the channel sampling duration, and f_D is the maximum Doppler shift [39]. $\Delta \boldsymbol{e}_{uk}[n+1]$ is an uncorrelated complex white Gaussian noise vector with its elements obeying the i.i.d. $\mathcal{CN}\left(0, \left(1-\rho^2\right)\sigma_{uk}^2\right)$.

After substituting (17) into (19), we can obtain

$$\begin{aligned}
\boldsymbol{h}_{uk}&[n+1] \\
&= \rho \boldsymbol{h}_{uk}[n] + \Delta \boldsymbol{e}_{uk}[n+1] \\
&= \rho\left[\rho \boldsymbol{h}_{uk}[n-1] + \Delta \boldsymbol{e}_{uk}[n]\right] + \Delta \boldsymbol{e}_{uk}[n+1] \\
&= \rho^2 \boldsymbol{h}_{uk}[n-1] + \rho \Delta \boldsymbol{e}_{uk}[n] + \Delta \boldsymbol{e}_{uk}[n+1] \\
&= \rho^{n+1}\boldsymbol{h}_{uk}[0] + \rho^n \Delta \boldsymbol{e}_{uk}[1] + \cdots + \rho \Delta \boldsymbol{e}_{uk}[n] \\
&\quad + \Delta \boldsymbol{e}_{uk}[n+1] \\
&= \rho^{n+1}\tilde{\boldsymbol{h}}_{uk}[0] + \rho^{n+1}\Delta \boldsymbol{h}_{uk}[0] + \tilde{\boldsymbol{e}}_{uk}[n+1],
\end{aligned} \tag{20}$$

where $\tilde{\boldsymbol{e}}_{uk}[n+1] = \sum_{i=0}^{n} \rho^i \Delta \boldsymbol{e}_{uk}[n+1-i]$, and $n = 0, 1, 2, \cdots$. We express

$$\boldsymbol{h}_{uk}[n] = \tilde{\boldsymbol{h}}_{uk}[n] + \boldsymbol{e}_{uk}(n), \tag{21}$$

where $\tilde{\boldsymbol{h}}_{uk}[n] = \rho^n \tilde{\boldsymbol{h}}_{uk}[0]$, $\boldsymbol{e}_{uk}(n) = \rho^n \Delta \boldsymbol{h}_{uk}[0] + \tilde{\boldsymbol{e}}_{uk}[n]$. It can be shown that each entry of $\boldsymbol{e}_{uk}(n)$ is a Gaussian random variable with zero mean and a variance of $\sigma_{e_{uk}}^2(n) = \sigma_{uk}^2 - \rho^{2n}\frac{\tau_u P_S \sigma_{uk}^4}{1+\tau_u P_S \sigma_{uk}^2}$. Consequently, when considering all the $2K$ users, $\boldsymbol{H}_u[n]$ can be expressed as

$$\boldsymbol{H}_u[n] = \rho^n \tilde{\boldsymbol{H}}_u[0] + \boldsymbol{E}_u[n], \tag{22}$$

where $\boldsymbol{E}_u[n] = \rho^n \Delta \boldsymbol{H}_u[0] + \tilde{\boldsymbol{E}}_u[n]$ with $\Delta \boldsymbol{H}_u[0] = [\Delta \boldsymbol{h}_{u1}[0], \Delta \boldsymbol{h}_{u2}[0], \cdots, \Delta \boldsymbol{h}_{u2K}[0]]$ and $\tilde{\boldsymbol{E}}_u[n] = \left[\tilde{\boldsymbol{e}}_{u1}[0], \tilde{\boldsymbol{e}}_{u2}[0], \cdots, \tilde{\boldsymbol{e}}_{u2K}[0]\right]$.

Similarly, when considering the downlink scenario, we have

$$\boldsymbol{h}_{dk}[n] = \tilde{\boldsymbol{h}}_{dk}[n] + \boldsymbol{e}_{dk}(n), \tag{23}$$

where $\tilde{\boldsymbol{h}}_{dk}[n] = \phi^n \tilde{\boldsymbol{h}}_{dk}[0]$, $\boldsymbol{e}_{dk}(n) = \phi^n \Delta \boldsymbol{h}_{dk}[0] + \tilde{\boldsymbol{e}}_{dk}[n]$ with ϕ denoting the correlation coefficient. Furthermore, the elements of $\boldsymbol{e}_{dk}(n)$ obey the i.i.d. $\mathcal{CN}(0, \sigma_{e_{dk}}^2(n))$ with $\sigma_{e_{dk}}^2(n) = \sigma_{dk}^2 - \phi^{2n}\frac{\tau_d P_R \sigma_{dk}^4}{1+\tau_d P_R \sigma_{dk}^2}$. Moreover, when considering all $2K$ downlink channels, we have

$$\boldsymbol{H}_d[n] = \phi^n \tilde{\boldsymbol{H}}_d[0] + \boldsymbol{E}_d[n], \tag{24}$$

where $\boldsymbol{E}_d[n] = \rho^n \Delta \boldsymbol{H}_d[0] + \tilde{\boldsymbol{E}}_d[n]$ with $\Delta \boldsymbol{H}_d[0] = [\Delta \boldsymbol{h}_{d1}[0], \Delta \boldsymbol{h}_{d2}[0], \cdots, \Delta \boldsymbol{h}_{d2K}[0]]$ and $\tilde{\boldsymbol{E}}_d[n] = [\tilde{\boldsymbol{e}}_{d1}[0], \tilde{\boldsymbol{e}}_{d2}[0], \cdots, \tilde{\boldsymbol{e}}_{d2K}[0]]$.

D. SPECTRAL-EFFICIENCY AND ENERGY-EFFICIENCY

In the FD relay systems, the system's SE during the transmission of the nth symbol can be expressed as

$$SE(n) = \mathbb{E}\left\{\sum_{k=1}^{2K} \log_2\left(1 + \gamma_k(n)\right)\right\}, \tag{25}$$

where the SINR is

$$\gamma_k(n) = \frac{P_k(n)}{P_I(n)}, \quad n = 1, 2, \cdots, \tag{26}$$

where $P_k(n)$ denotes the power of the desired signal, while $P_I(n)$ denotes the total power of channel estimation errors, interference and noise.

Accordingly, the EE can be evaluated as the ratio between the system's SE and the total power consumption of the system, written as

$$EE(n) = \frac{SE(n)}{P_{total}}, \tag{27}$$

where P_{total} is the total power consumption at all the users and at the relay, which is given by $P_{total} = 2KP_S + P_R$, according to our previous consumptions in Section II-A.

Note that, information exchange between pairs of users in Fig. 1 needs two phases in the HD relay systems. Correspondingly, the SE of the HD relay systems can be expressed as

$$SE^{HD}(n) = \frac{1}{2}\mathbb{E}\left\{\sum_{k=1}^{2K} \log_2\left(1 + \gamma_k(n)\right)\right\}, \tag{28}$$

where $\gamma_k(n)$ can be derived from the formula (11).

III. ASYMPTOTIC SPECTRAL-EFFICIENCY AND ENERGY-EFFICIENCY WITH CHANNEL AGING

In this section, we analyze the SE and EE performance of the MTW-MMR systems with MRC/MRT or ZFR/ZFT assisted relay processing, when four proposed power-scaling schemes are respectively considered, associated with taking into account of the channel aging effect.

A. MRC/MRT RELAY PROCESSING

At the relay, the MRC/MRT processing matrix can be derived to be [18]

$$\boldsymbol{W}_{mr} = \underbrace{\boldsymbol{H}_d^*}_{MRT} \boldsymbol{T} \underbrace{\boldsymbol{H}_u^H}_{MRC}, \tag{29}$$

where $\boldsymbol{T} = \mathrm{diag}(\boldsymbol{T}_1, \boldsymbol{T}_2, \cdots \boldsymbol{T}_K)$, $\boldsymbol{T}_m = \begin{bmatrix} 0 & 1 \\ 1 & 0 \end{bmatrix}$, $m = 1, 2, \cdots, K$. When channel estimation and channel aging are involved for the nth symbol, the amplification matrix $\boldsymbol{W}_R(n)$ in (3) can be derived as

$$\boldsymbol{W}_R(n) = \alpha(n)\tilde{\boldsymbol{W}}_{mr}(n) = \tilde{\alpha}(n)\tilde{\boldsymbol{W}}_{mr}(0), \tag{30}$$

where $\tilde{\alpha}(n) = (\rho\phi)^n \alpha(n)$, and $\tilde{\boldsymbol{W}}(0)$ is given by

$$\tilde{\boldsymbol{W}}_{mr}(0) = \tilde{\boldsymbol{H}}_d^*(0)\boldsymbol{T}\tilde{\boldsymbol{H}}_u^H(0). \tag{31}$$

Based on [50, Lemma 1], for $N \to \infty$, we can obtain

$$\frac{\tilde{\boldsymbol{h}}_{dk}^{T}(0)\,\tilde{\boldsymbol{W}}_{mr}(0)\,\tilde{\boldsymbol{h}}_{uk'}(0)}{N^{2}} \to \begin{cases} \hat{\sigma}_{dk}^{2}\hat{\sigma}_{uk'}^{2} & j=k', \\ 0 & j\neq k', \end{cases} \tag{32}$$

which implies that the inter-pair interference given by those users with $j \neq k, k'$ and the self-interference for $j = k$ can be effectively eliminated, as $N \to \infty$.

B. ZFR/ZFT RELAY PROCESSING

For the ZFR/ZFT relay processing, the processing matrix can be given as [49]

$$\boldsymbol{W}_{zf} = \underbrace{\boldsymbol{H}_{d}^{*}\left(\boldsymbol{H}_{d}^{T}\boldsymbol{H}_{d}^{*}\right)^{-1}}_{ZFT}\boldsymbol{T}\underbrace{\left(\boldsymbol{H}_{u}^{H}\boldsymbol{H}_{u}\right)^{-1}\boldsymbol{H}_{u}^{H}}_{ZFR}. \tag{33}$$

Hence, for the nth symbol, the amplification matrix $\boldsymbol{W}_{R}(n)$ seen in (3) can be expressed as

$$\boldsymbol{W}_{R}(n) = \alpha(n)\,\tilde{\boldsymbol{W}}_{zf}(n) = \tilde{\alpha}(n)\,\tilde{\boldsymbol{W}}_{zf}(0), \tag{34}$$

with $\tilde{\alpha}(n) = \frac{1}{(\rho\phi)^{n}}\alpha(n)$, and $\tilde{\boldsymbol{W}}_{zf}(0)$ given by

$$\tilde{\boldsymbol{W}}_{zf}(0) = \tilde{\boldsymbol{H}}_{d}^{*}(0)\left(\tilde{\boldsymbol{H}}_{d}^{T}(0)\,\tilde{\boldsymbol{H}}_{d}^{*}(0)\right)^{-1}\boldsymbol{T} \times \left(\tilde{\boldsymbol{H}}_{u}^{H}(0)\,\tilde{\boldsymbol{H}}_{u}(0)\right)^{-1}\tilde{\boldsymbol{H}}_{u}^{H}(0). \tag{35}$$

When channel estimation and channel aging are considered, explicitly, we have $\tilde{\boldsymbol{H}}_{d}^{T}(0)\,\tilde{\boldsymbol{W}}_{zf}(0)\,\tilde{\boldsymbol{H}}_{u}(0) = \boldsymbol{T}$, hence

$$\tilde{\boldsymbol{h}}_{dk}^{T}(0)\,\tilde{\boldsymbol{W}}_{zf}(0)\,\tilde{\boldsymbol{h}}_{uj}(0) = \begin{cases} 1 & j=k', \\ 0 & j\neq k', \end{cases} \tag{36}$$

which means that all the inter-pair interference and self-interference are completely removed.

C. SPECTRAL-EFFICIENCY AND ENERGY-EFFICIENCY OF MTW-MMR SYSTEMS WITH DIFFERENT POWER SCALING SCHEMES

In this subsection, we derive the expressions for the SE and EE of the MTW-MMR systems, when four power scaling schemes are respectively considered. In general, the power scaling rules can be represented as $P_S = E_S/N^a$ and $P_R = E_R/N^b$ with $0 \leqslant a, b \leqslant 1$, where E_S and E_R are fixed values. Different power scaling rules correspond to the different values of a and b, as shown below.

1) CASE 1: $P_S = E_S$, $P_R = E_R$

In the context of Case 1, $a = b = 0$, giving $P_S = E_S$ and $P_R = E_R$. Under this power scaling rule, both the transmit power of the users and the transmit power of the relay are not changed, as the number of antennas of the relay increases or decreases. Under this operational scenario, the SE and EE of the MTW-MMR systems employing the MRC/MRT and ZFR/ZFT relay processing are given by the following two theorems, respectively.

Theorem 1: There exists at least one Nash equilibrium for the differential game.

Assuming the MRC/MRT relay processing based on the aged CSI, the asymptotic SE and EE of the MTW-MMR systems can be expressed as

$$SE_{mr}^{FD}(n) = 2K\cdot\log_{2}\left(1+\frac{\rho^{2(n-1)}\phi^{2n}E_{S}\left(\hat{\sigma}_{dk}^{2}\hat{\sigma}_{uk'}^{2}\right)^{2}}{E_{S}a_{mr}+E_{R}b_{mr}}\right), \tag{37}$$

$$EE_{mr}^{FD}(n) = \frac{2K\cdot\log_{2}\left(1+\frac{\rho^{2(n-1)}\phi^{2n}E_{S}\left(\hat{\sigma}_{dk}^{2}\hat{\sigma}_{uk'}^{2}\right)^{2}}{E_{S}a_{mr}+E_{R}b_{mr}}\right)}{2K\cdot E_{S}+E_{R}}, \tag{38}$$

$$SE_{mr}^{HD}(n) = K\cdot\log_{2}\left(1+\frac{\rho^{2(n-1)}\phi^{2n}\left(\hat{\sigma}_{dk}^{2}\hat{\sigma}_{uk'}^{2}\right)^{2}}{a_{mr}}\right), \tag{39}$$

$$EE_{mr}^{HD}(n) = \frac{K\cdot\log_{2}\left(1+\frac{\rho^{2(n-1)}\phi^{2n}\left(\hat{\sigma}_{dk}^{2}\hat{\sigma}_{uk'}^{2}\right)^{2}}{a_{mr}}\right)}{2K\cdot E_{S}+E_{R}}, \tag{40}$$

for $n = 1, 2, \cdots$.

Proof 1: See Appendix A.

In the above formulas, the term $P_S a_{mr}$ denotes the channel estimation errors, and the term $P_R b_{mr}$ denotes the self-loop interference on the relay. From (37) and (38), we observe that in the FD-assisted MTW-MMR systems, the self-loop interference and inter-user interference on a user, as well as the noise on the relay and users can be successfully removed by employing a big number of antennas at the relay, while the channel estimation errors and self-loop interference on the relay still exist. By contrast, as seen in (39) and (40) in the HD systems, the self-loop interference on the relay disappears, as $N \to \infty$.

Theorem 2: When the ZFR/ZFT relay processing based on aged CSI is employed, the asymptotic SE and EE of the MTW-MMR systems for $n = 1, 2, \cdots$ are given by

$$SE_{zf}^{FD}(n) = 2K\cdot\log_{2}\left(1+\frac{\rho^{2(n-1)}\phi^{2n}E_{S}}{E_{S}a_{zf}+E_{R}b_{zf}}\right), \tag{41}$$

$$EE_{zf}^{FD}(n) = \frac{2K\cdot\log_{2}\left(1+\frac{\rho^{2(n-1)}\phi^{2n}E_{S}}{E_{S}a_{zf}+E_{R}b_{zf}}\right)}{2K\cdot E_{S}+E_{R}}, \tag{42}$$

$$SE_{zf}^{HD}(n) = K\cdot\log_{2}\left(1+\frac{\rho^{2(n-1)}\phi^{2n}}{a_{zf}}\right), \tag{43}$$

$$EE_{zf}^{HD}(n) = \frac{K\cdot\log_{2}\left(1+\frac{\rho^{2(n-1)}\phi^{2n}}{a_{zf}}\right)}{2K\cdot E_{S}+E_{R}}. \tag{44}$$

Proof 2: See Appendix B. □

In the above formulas, with the case of ZFR/ZFT relay processing, the term $P_S a_{zf}$ denotes the channel estimation errors, and the term $P_R b_{zf}$ denotes the self-loop interference on the relay. When comparing (41)-(44) correspondingly with (37)-(40), we can find that in Case 1, the asymptotic SE and EE of the MTW-MMR systems employing ZFR/ZFT processing have similar forms as that of the MTW-MMR systems with MRC/MRT processing. As shown in (41)-(44), both the SE and EE decrease as the uplink channel correlation coefficient ρ or the downlink channel correlation coefficient

ϕ decreases. This is because, as the channels become less correlated, or the channel aging effect becomes severer, the CSI estimated at $t = 0$ becomes less reliable at time n increases, and hence, resulting in the loss of SE and EE.

2) CASE 2: $P_S = E_S$, $P_R = E_R/N$

For Case 2 of power scaling, we have $a = 0$ and $b = 1$. This corresponds to the operational scenario where the transmit power of a user does not change, regardless of the number of antennas deployed at the relay. By contrast, the transmit power of the relay is linearly decreased with the increase of the number of antennas deployed at the relay.

Theorem 3: When channel aging is considered, the asymptotic SE and EE of the MTW-MMR systems employing the MRC/MRT relay processing can be expressed as

$$SE_{mr}^{FD}(n) = 2K \cdot \log_2 \left(1 + \frac{\rho^{2(n-1)}\phi^{2n}E_R\left(\hat{\sigma}_{dk}^2\hat{\sigma}_{uk'}^2\right)^2}{E_R a_{mr} + \rho^{2(n-1)}\sum_{i=1}^{2K}\hat{\sigma}_{di}^2\hat{\sigma}_{ui'}^4\left(\sum_{i,k\in U_k}\sigma_{k,i}^2E_S + \sigma_n^2\right)}\right), \tag{45}$$

$$EE_{mr}^{FD}(n) = \frac{\log_2\left(1 + \frac{\rho^{2(n-1)}\phi^{2n}E_R\left(\hat{\sigma}_{dk}^2\hat{\sigma}_{uk'}^2\right)^2}{E_R a_{mr} + \rho^{2(n-1)}\sum_{i=1}^{2K}\hat{\sigma}_{di}^2\hat{\sigma}_{ui'}^4\left(\sum_{i,k\in U_k}\sigma_{k,i}^2E_S + \sigma_n^2\right)}\right)}{E_S}, \tag{46}$$

$$SE_{mr}^{HD}(n) = K \cdot \log_2\left(1 + \frac{\rho^{2(n-1)}\phi^{2n}E_R\left(\hat{\sigma}_{dk}^2\hat{\sigma}_{uk'}^2\right)^2}{E_R a_{mr} + \rho^{2(n-1)}\sum_{i=1}^{2K}\hat{\sigma}_{di}^2\hat{\sigma}_{ui'}^4\sigma_n^2}\right), \tag{47}$$

$$EE_{mr}^{HD}(n) = \frac{\log_2\left(1 + \frac{\rho^{2(n-1)}\phi^{2n}E_R\left(\hat{\sigma}_{dk}^2\hat{\sigma}_{uk'}^2\right)^2}{E_{Rmr}a + \rho^{2(n-1)}\sum_{i=1}^{2K}\hat{\sigma}_{di}^2\hat{\sigma}_{ui'}^4\sigma_n^2}\right)}{2E_S}, \tag{48}$$

for $n = 1, 2, \cdots$.

Proof 3: See Appendix C. □

From (45)-(46), we can observe that, in the FD mode, the self-loop interference and noise reflected by the relay can be effectively removed, as N approaches infinity. However, the channel estimation errors, noise from user k, self-loop interference and inter-user interference on user k cannot be mitigated. This is because, in Case 2, the transmit power of a user remains constant, while the transmit power of the relay is decreased with the increase of the number of antennas at the relay. As the transmit power sent by the relay becomes lower and lower, the power of the users becomes so strong, which results in the severe self-loop interference and inter-user interference, that cannot be removed by employing a large number of antennas at the relay. By contrast, when operated in the HD mode as shown in (47)-(48), the self-loop interference and inter-user interference on user k can be removed in comparison to that in (45)-(46), owing to the transmission characteristics in the HD mode.

Theorem 4: When the ZFR/ZFT relay processing based on aged CSI is employed, the asymptotic SE and EE of the MTW-MMR systems operated in Case 2 are given by

$$SE_{zf}^{FD}(n) = 2K \cdot \log_2 \times \left(1 + \frac{\rho^{2(n-1)}\phi^{2n}E_R}{E_R a_{zf} + \rho^{2(n-1)}\sum_{i=1}^{2K}\frac{1}{\hat{\sigma}_{di}}\left(\sum_{i,k\in U_k}\sigma_{k,i}^2E_S + \sigma_n^2\right)}\right), \tag{49}$$

$$EE_{zf}^{FD}(n) = \frac{\log_2\left(1 + \frac{\rho^{2(n-1)}\phi^{2n}E_R}{E_R a_{zf} + \rho^{2(n-1)}\sum_{i=1}^{2K}\frac{1}{\hat{\sigma}_{di}}\left(\sum_{i,k\in U_k}\sigma_{k,i}^2E_S + \sigma_n^2\right)}\right)}{E_S}, \tag{50}$$

$$SE_{zf}^{HD}(n) = K \cdot \log_2\left(1 + \frac{\rho^{2(n-1)}\phi^{2n}E_R}{E_R a_{zf} + \rho^{2(n-1)}\sum_{i=1}^{2K}\frac{1}{\hat{\sigma}_{di}}\sigma_n^2}\right), \tag{51}$$

$$EE_{zf}^{HD}(n) = \frac{\log_2\left(1 + \frac{\rho^{2(n-1)}\phi^{2n}E_R}{E_R a_{zf} + \rho^{2(n-1)}\sum_{i=1}^{2K}\frac{1}{\hat{\sigma}_{di}}\sigma_n^2}\right)}{2E_S}, \tag{52}$$

for $n = 1, 2, \cdots$.

Proof 4: See Appendix D. □

When comparing (49)-(52) with (45)-(48), we can see that the SE and EE expressions under the ZFR/ZFT relay processing are similar to that under the MRC/MRT relay processing. In (49)-(50), the self-loop interference and noise on the relay can be removed owing to the effect of massive antennas at the relay. Moreover, in (50) and (52), we observe that the transmit power of the users becomes a factor limiting the EE. This is because the transmit power of the relay decreases making the impact of P_R on the EE become less important, while P_S on the EE becomes dominant.

3) CASE 3: $P_S = E_S/N$, $P_R = E_R/N$

In Case 3, both the transmit power of a mobile user and the transmit power of the relay are linearly scaled down, as the

$$SE_{mr}^{FD}(n) = 2K \cdot \log_2\left(1 + \frac{\rho^{2(n-1)}\phi^{2n}E_R E_S\left(\hat{\sigma}_{dk}^2\hat{\sigma}_{uk'}^2\right)^2}{E_R E_S a_{mr} + E_R^2 b_{mr} + \sigma_{nr}^2 E_R d_{mr} + E_S\sigma_n^2\rho^{2(n-1)}\sum_{i=1}^{2K}\hat{\sigma}_{di}^2\hat{\sigma}_{ui'}^4}\right), \tag{53}$$

$$EE_{mr}^{FD}(n) = \frac{N \cdot 2K \cdot \log_2\left(1 + \frac{\rho^{2(n-1)}\phi^{2n}E_R E_S\left(\hat{\sigma}_{dk}^2\hat{\sigma}_{uk'}^2\right)^2}{E_R E_S a_{mr} + E_R^2 b_{mr} + \sigma_{nr}^2 E_R d_{mr} + E_S\sigma_n^2\rho^{2(n-1)}\sum_{i=1}^{2K}\hat{\sigma}_{di}^2\hat{\sigma}_{ui'}^4}\right)}{2K \cdot E_S + E_R}, \tag{54}$$

$$SE_{mr}^{HD}(n) = K \cdot \log_2\left(1 + \frac{\rho^{2(n-1)}\phi^{2n}E_R E_S\left(\hat{\sigma}_{dk}^2\hat{\sigma}_{uk'}^2\right)^2}{E_R E_S a_{mr} + \sigma_{nr}^2 E_R d_{mr} + E_S\sigma_n^2\rho^{2(n-1)}\sum_{i=1}^{2K}\hat{\sigma}_{di}^2\hat{\sigma}_{ui'}^4}\right), \tag{55}$$

$$EE_{mr}^{HD}(n) = \frac{N \cdot K \cdot \log_2\left(1 + \frac{\rho^{2(n-1)}\phi^{2n}E_R E_S\left(\hat{\sigma}_{dk}^2\hat{\sigma}_{uk'}^2\right)^2}{E_R E_S a_{mr} + \sigma_{nr}^2 E_R d_{mr} + E_S\sigma_n^2\rho^{2(n-1)}\sum_{i=1}^{2K}\hat{\sigma}_{di}^2\hat{\sigma}_{ui'}^4}\right)}{2K \cdot E_S + E_R}, \tag{56}$$

number of antennas at the relay increases. Therefore, we have $a = b = 1$. In this case, the SE and EE of the MTW-MMR systems in FD or HD mode are given by the following two theorems.

Theorem 5: When the MRC/MRT relay processing based on aged CSI is employed, the asymptotic SE and EE of the MTW-MMR systems can be expressed as (53)–(56), as shown at the top of this page, for $n = 1, 2, \cdots$.

Proof 5: See Appendix E.

As shown in (53), when the MTW-MMR system is operated in Case 3, only the self-loop interference and inter-user interference on the users can be eliminated, when $N \to \infty$. By contrast, when operated in Case 1, as shown in (37), the noise from the relay and from user k, self-loop interference and inter-user interference on user k can all be removed, as $N \to \infty$. Consequently, the SE of the MTW-MMR system in Case 3 is smaller than that of the MTW-MMR system in Case 1. In terms of the EE of Case 3, the transmit power of the relay P_R and that of the users P_S decrease with the increase of the number of antennas at the relay. Hence, it is shown that the EE increases as P_S and P_R decrease. Furthermore, when the number of antennas at the relay increases, the EE increases linearly, leading to $EE_{mr}^{FD}(n) \to \infty$ and $EE_{mr}^{HD}(n) \to \infty$, as $N \to \infty$.

Theorem 6: When the ZFR/ZFT relay processing based on aged CSI is employed, the asymptotic SE and EE of the MTW-MMR system can be expressed as

for $n = 1, 2, \cdots$.

Proof 6: See Appendix F. □

In the case of ZFR/ZFT relay processing, we observe that the asymptotic SE and EE of the MTW-MMR systems under the ZFR/ZFT processing as shown in (57)-(60), as shown at the top of the next page, are similar with that under the MRC/MRT relay processing shown in (53)-(56). The EE in (58) and (60) tend to infinity, when N approaches infinity, for the similar reason explained for (54) and (56). Therefore, we can draw the conclusion that the EE in Case 3 is the largest among the four cases considered, as shown in Fig. 5 in Section IV.

4) CASE 4: $P_S = E_S/N$, $P_R = E_R$

In this power scaling case, we set $a = 1$ and $b = 0$. Therefore, the transmit power of a user linearly scales down with N increasing, while the transmit power of the relay remains constant, regardless of the number of antennas employed by the relay. In this case, the SE and EE of the MTW-MMR systems with MRC/MRT and ZFR/ZFT relay processing are summarized by Theorems 7 and 8, respectively.

Theorem 7: When the MRC/MRT relay processing based on aged CSI is employed, the asymptotic SE and EE of the MTW-MMR system can be expressed as

$$SE_{mr}^{FD}(n) = 2K \cdot \log_2\left(1 + \frac{\rho^{2(n-1)}\phi^{2n}E_S\left(\hat{\sigma}_{dk}^2\hat{\sigma}_{uk'}^2\right)^2}{E_S a_{mr} + N E_R b_{mr} + \sigma_{nr}^2 d_{mr}}\right), \tag{61}$$

$$EE_{mr}^{FD}(n) = \frac{2K \cdot \log_2\left(1 + \frac{\rho^{2(n-1)}\phi^{2n}E_S\left(\hat{\sigma}_{dk}^2\hat{\sigma}_{uk'}^2\right)^2}{E_S a_{mr} + N E_R b_{mr} + \sigma_{nr}^2 d_{mr}}\right)}{E_R}, \tag{62}$$

$$SE_{mr}^{HD}(n) = K \cdot \log_2\left(1 + \frac{\rho^{2(n-1)}\phi^{2n}E_S\left(\hat{\sigma}_{dk}^2\hat{\sigma}_{uk'}^2\right)^2}{E_S a_{mr} + \sigma_{nr}^2 d_{mr}}\right), \tag{63}$$

$$SE_{zf}^{FD}(n) = 2K \cdot \log_2\left(1+\frac{\rho^{2(n-1)}\phi^{2n}E_SE_R}{E_SE_Ra_{zf}+E_R^2b_{zf}+\sigma_{nr}^2E_Rd_{zf}+E_S\sigma_n^2\rho^{2(n-1)}\sum_{i=1}^{2K}\frac{1}{\hat{\sigma}_{di}}}\right), \tag{57}$$

$$EE_{zf}^{FD}(n) = \frac{N\cdot 2K \cdot \log_2\left(1+\frac{\rho^{2(n-1)}\phi^{2n}E_SE_R}{E_SE_Ra_{zf}+E_R^2b_{zf}+\sigma_{nr}^2E_Rd_{zf}+E_S\sigma_n^2\rho^{2(n-1)}\sum_{i=1}^{2K}\frac{1}{\hat{\sigma}_{di}}}\right)}{2K\cdot E_S+E_R}, \tag{58}$$

$$SE_{zf}^{HD}(n) = K \cdot \log_2\left(1+\frac{\rho^{2(n-1)}\phi^{2n}E_SE_R}{E_SE_Ra_{zf}+\sigma_{nr}^2E_Rd_{zf}+E_S\sigma_n^2\rho^{2(n-1)}\sum_{i=1}^{2K}\frac{1}{\hat{\sigma}_{di}}}\right), \tag{59}$$

$$EE_{zf}^{HD}(n) = \frac{N\cdot K \cdot \log_2\left(1+\frac{\rho^{2(n-1)}\phi^{2n}E_SE_R}{E_SE_Ra_{zf}+\sigma_{nr}^2E_Rd_{zf}+E_S\sigma_n^2\rho^{2(n-1)}\sum_{i=1}^{2K}\frac{1}{\hat{\sigma}_{di}}}\right)}{2K\cdot E_S+E_R}, \tag{60}$$

$$EE_{mr}^{HD}(n) = \frac{K\cdot\log_2\left(1+\frac{\rho^{2(n-1)}\phi^{2n}E_S\left(\hat{\sigma}_{dk}^2\hat{\sigma}_{uk'}^2\right)^2}{E_Sa_{mr}+\sigma_{nr}^2d_{mr}}\right)}{E_R}, \tag{64}$$

for $n = 1, 2, \cdots$.

Proof 7: See Appendix G.

In the FD mode, as shown in (61), the SE decreases, as the transmit/receive antennas at the relay N increases. When $N \to \infty$, it can be shown that $SE_{mr}^{FD}(n) \to 0$, resulting in that $EE_{mr}^{FD}(n) \to 0$. The SE decreases with the $\gamma_k(n) = \frac{P_k(n)}{P_I(n)}$ decreasing, in this case, when N increases, the transmit power of the users decrease, leading to the decrease of $P_k(n)$, therefore, the SE approaches 0 when $N \to \infty$ in Case 4. By contrast, in the HD mode, the self-loop interference on the relay, the self-loop interference, inter-user interference and noise at the user k can be effectively removed, only the noise at the relay and channel estimation errors remain in (63), as $N \to \infty$.

Theorem 8: When the ZFR/ZFT relaying processing based on the aged CSI is employed, the asymptotic SE and EE of the MTW-MMR system can be expressed as

$$SE_{zf}^{FD}(n) = 2K\cdot\log_2\left(1+\frac{\rho^{2(n-1)}\phi^{2n}E_S}{E_Sa_{zf}+NE_Rb_{zf}+\sigma_{nr}^2d_{zf}}\right), \tag{65}$$

$$EE_{zf}^{FD}(n) = \frac{2K\cdot\log_2\left(1+\frac{\rho^{2(n-1)}\phi^{2n}E_S}{E_Sa_{zf}+NE_Rb_{zf}+\sigma_{nr}^2d_{zf}}\right)}{E_R}, \tag{66}$$

$$SE_{zf}^{HD}(n) = K\cdot\log_2\left(1+\frac{\rho^{2(n-1)}\phi^{2n}E_S}{E_Sa_{zf}+\sigma_{nr}^2d_{zf}}\right), \tag{67}$$

$$EE_{zf}^{HD}(n) = \frac{K\cdot\log_2\left(1+\frac{\rho^{2(n-1)}\phi^{2n}E_S}{E_Sa_{zf}+\sigma_{nr}^2d_{zf}}\right)}{E_R}, \tag{68}$$

for $n = 1, 2, \cdots$.

Proof 8: See Appendix H. □

In this case, the expressions of SE and EE as shown in (65)-(68) are similar with that shown in (61)-(64). It is shown that $SE_{zf}^{FD}(n) \to 0$ and $EE_{zf}^{FD}(n) \to 0$ due to the big number of antennas at the relay in the FD mode. In comparison to (67)-(68) in the HD mode, we can learn that the SE and EE in Case 4 of the HD mode are larger than the corresponding SE and EE in the FD mode, when N approaches infinity.

D. SPECTRAL-EFFICIENCY AND ENERGY-EFFICIENCY COMPARISON BETWEEN DIFFERENT POWER SCALING SCHEMES

In this subsection, we summarize the characteristics of the four proposed power scaling schemes. For convenience of comparison, we show a table as Table 1 to depict the differences. Note that, since the SE and EE under the MRC/MRT relay processing and the ZFR/ZFT relay processing are very similar, with $N \to \infty$. Hence, they are considered together without distinction in Table I.

IV. PERFORMANCE RESULTS

In this section, we present the simulation results for the MTW-MMR systems with the four proposed power scaling schemes. In our simulations, we assume that $P_S = 20$dB, $P_R = 27$dB, $\sigma_{uk}^2 = \sigma_{dk}^2 = \sigma_{nr}^2 = \sigma_n^2 = 1$, and $\sigma_{RR}^2 = \sigma_{k,i}^2 = 0.01$. Besides, we assume that the temporal correlation parameters reflecting channel aging satisfy $\rho = \phi$ for convenience.

TABLE 1. characteristics of the Spectral-Efficiency and Energy-Efficiency of The Four Power Scaling Cases.

Cases	$SE^{FD}(n)$	$SE^{HD}(n)$	$EE^{FD}(n)$	$EE^{HD}(n)$
Case 1	Self-loop interference and inter -user interference on a user, noise on the relay and users are removed. The SE in Case 1 is the largest in the four cases.	Self-loop interference on the relay is removed.	Only channel estimation errors and self-loop interference on the relay remain.	Only channel estimation errors remains.
Case 2	Self-loop interference and noise on the relay are removed.	Self-loop interference and inter-user interference on user k are removed.	Channel estimation errors, noise from user k, self-loop interference and inter-user interference on user k remain.	Channel estimation errors and noise from user k remain.
Case 3	Only self-loop interference and inter-user interference on the users are removed.	Self-loop interference on the relay and users, inter-user interference are removed.	$EE^{FD}(n) \to \infty$ with $N \to \infty$.	$EE^{HD}(n) \to \infty$ with $N \to \infty$.
Case 4	$SE^{FD}(n) \to 0$ with $N \to \infty$.	Self-loop interference on the relay, self-loop interference, inter-user interference and noise on user k are removed.	$EE^{FD}(n) \to 0$ with $N \to \infty$.	Only channel estimation errors and noise at the relay remain.

A. SPECTRAL-EFFICIENCY

As shown in Fig. 2 (a) and Fig. 2 (b), the SE of the FD-assisted MTW-MMR systems in Cases 1 $\sim$ 4 with the MRC/MRT or ZFR/ZFT relay processing is depicted. Firstly, given the MRC/MRT or ZFR/ZFT relay processing, we observe that the SE in Case 1 is the largest among the four cases, and the SE grows with the increase of N. By contrast, in Case 4, the SE approaches 0, as N increases, which is in consistent with the theoretical results obtained through analysis in Section III. As seen in Fig. 2, in Case 2 and 3, the SE first increases and then decreases, as N increases. This is because, when the transmit power at the relay is scaled down to $1/N$, the number of relay antennas is the principal factor determining the achievable SE. However, when N exceeds a certain value, $\hat{\sigma}_{di}^2$ associated with the downlink channel estimation becomes more and more unreliable, due to the reduction of transmit power at the relay, which leads to the decrease of SE. In addition, we can see that the SE in Case 3 is larger than the corresponding SE in Case 2.

Secondly, for the same case, it is shown that the SE of the FD-assisted MTW-MMR systems with ZFR/ZFT relay processing is superior to that of the FD-assisted MTW-MMR systems with MRC/MRT relay processing. This is because inter-pair interference and self-interference can be effectively mitigated by the ZFR/ZFT relay processing, which is not the case when the MRC/MRT relay processing is employed. Finally, the SE difference between the MRC/MRT and ZFR/ZFT relay processing schemes gradually converges, when the number of relay antennas N increases. The reason behind is that the inter-pair interference and self-interference under the MRC/MRT relay processing disappear, as $N \to \infty$.

Fig. 3 depicts the effect of channel aging on the SE of the FD-assisted MTW-MMR systems employing the MRC/MRT relay processing operated in the Cases 1 $\sim$ 4. Explicitly, the SE for a given case increases, when the temporal correlation parameter ρ increases, reflecting that the channel aging becomes less severe. This is the result that, when the temporal correlation parameter increases, the channels become more correlated, making their estimation more reliable, and we can see that, with the ρ increases, the SE grows faster since the impact of channel aging is decreasing. Furthermore, from a quantitative perspective, we can see that in Fig. 3, the SE degrades about 0.6dB when the temporal correlation parameter ρ changes from 1 to 0.9 for Cases 1, the SE degrades about 2.3dB for Case 2, and the SE degrades about 1.2dB for Case 3, when $\rho = 1$, it means that there exists only channel estimation but no channel aging, thus, in this case, the SE will be larger than that in $\rho = 0.9$.

In Fig. 4, we study the SE of the FD-assisted MTW-MMR systems versus the number of user pairs K in the cases of 1 $\sim$ 3, when the MRC/MRT or ZFR/ZFT relay processing is considered. It is apparent that the SE in Case 1 is the highest, while that in Case 2 is the lowest among the three cases. Furthermore, the SE in Case 2 tends to 0, as K increases, resulted from the severer inter-user interference under this circumstance. Additionally, we observe that the SE in Case 1, Case 2 and Case 3 first increases and then decreases as K increases. This is because, when K is small, the multiplexing gain dominates the achievable SE. However, when K further increases, the effect of interference becomes severe, which results in the loss of SE.

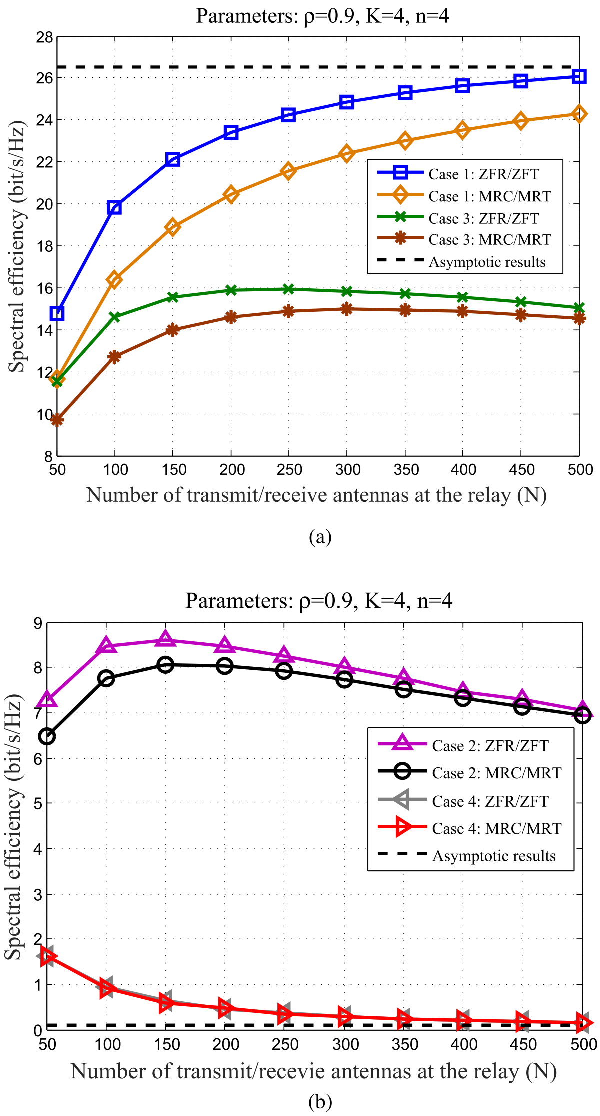

FIGURE 2. **Spectral-efficiency versus N of the MTW-MMR systems employing the FD relay under MRC/MRT or ZFR/ZFT relay processing.**

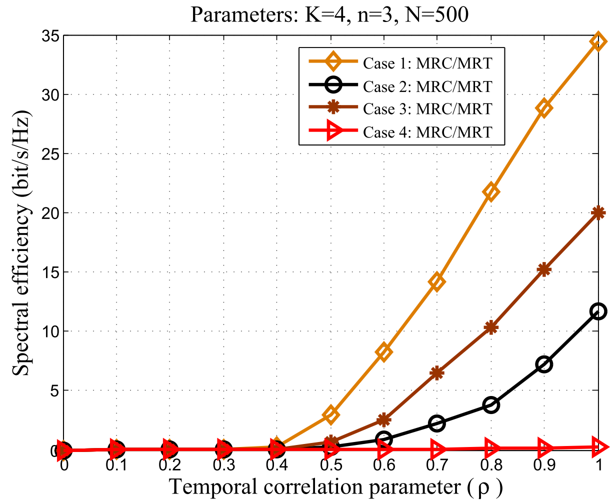

FIGURE 3. **Spectral-efficiency versus ρ of the MTW-MMR systems employing the FD relay operated under the MRC/MRT processing.**

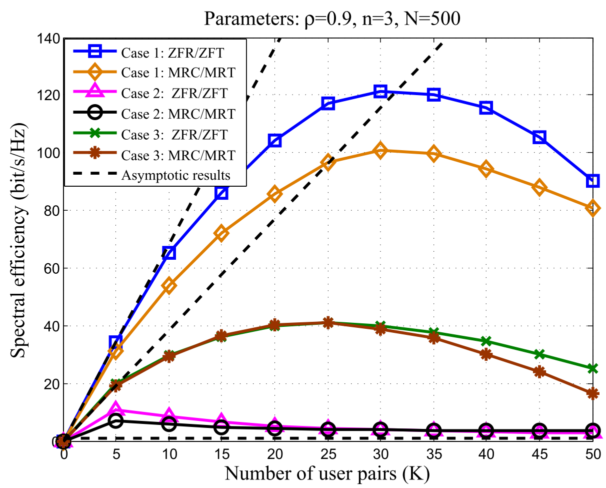

FIGURE 4. **Spectral-efficiency versus K of the MTW-MMR systems employing the FD relay operated under the MRC/MRT processing.**

B. ENERGY-EFFICIENCY

In Fig. 5 (a) and Fig. 5 (b), the EE of the FD-assisted MTW-MMR systems in the Cases 1 $\sim$ 4 with MRC/MRT or ZFR/ZFT relay processing is depicted. As seen in Fig. 5(a), the EE in Case 1 is larger than that in Case 2, and the EE in Case 4 is lower than that in Case 2, and approaches 0, as $N \rightarrow \infty$, which in line with the SE shown in Fig. 2. Furthermore, the tendency of EE in Cases 1, 2 and 4 is the same as the SE shown in Fig. 2. As shown in Fig. 5 (b), the EE in Case 3 is the largest among the four cases, owing to the transmit power of both the relay and the users are scaled down to $1/N$, leading to the increase of EE. Here, in conjunction with the SE shown in Fig. 2, we can draw the conclusion that the FD-assisted MTW-MMR system in Case 3 is capable of attaining the best performance tradeoff between SE and EE.

Fig. 6 shows the impact of channel aging on the EE of the FD-assisted MTW-MMR systems, when the ZFR/ZFT relay processing is considered. It is apparent that the EE increases, as the temporal correlation increases, as the result that more reliable channel estimation is attainable. In addition, it is shown that in Fig. 6, the EE degrades about 0.8dB when the temporal correlation parameter ρ changes from 1 to 0.9 for Case 1, the EE degrades about 1.7dB for Case 2, and the EE degrades about 1.2dB for Case 3. Similarly to the Fig. 3, the EE grow faster with the ρ becomes larger, and when ρ grows to 1, the channel aging impact can be ignored.

C. COMPARISON BETWEEN FULL-DUPLEX AND HALF-DUPLEX MODES

In the HD mode, the MTW-MMR system needs two time slots to complete one symbol exchange between a pair of users,

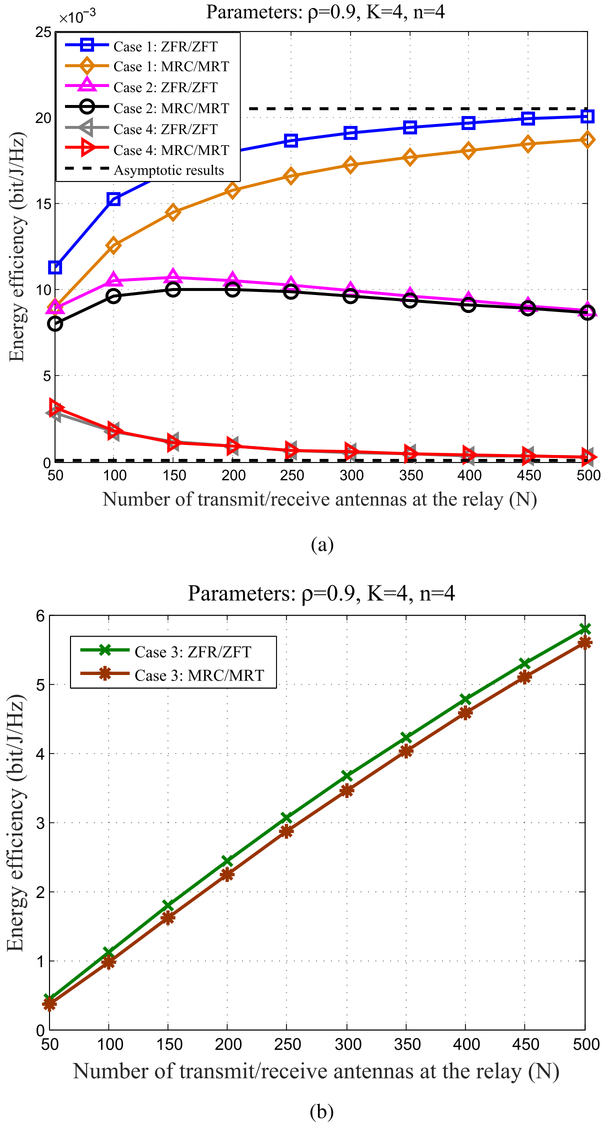

FIGURE 5. Energy-efficiency of the FD-assisted MTW-MMR systems under MRC/MRT or ZFR/ZFT principles.

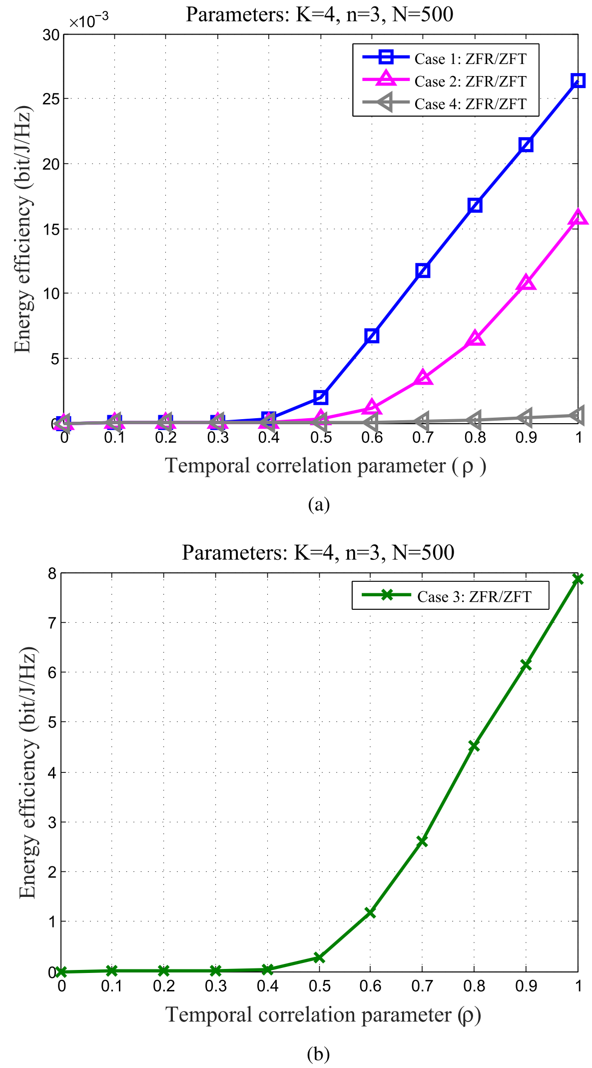

FIGURE 6. Energy-efficiency versus ρ of the FD-assisted MTW-MMR system under ZFR/ZFT processing.

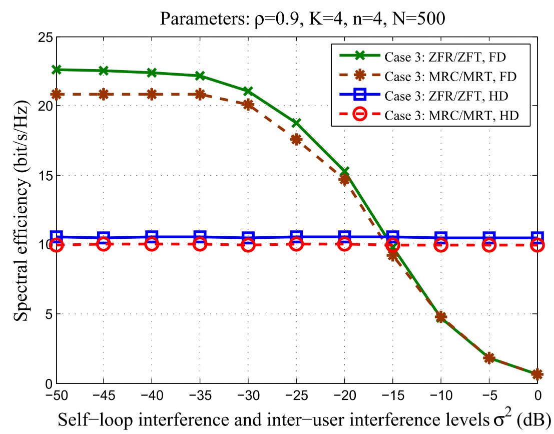

FIGURE 7. Spectral-efficiency versus the power of self-loop interference and inter-user interference for both FD and HD relay.

while only one time slot is required in the FD mode. However, the self-loop interference and inter-user interference existing in the FD-assisted MTW-MMR system do not exist in the HD-assisted MTW-MMR system. In Fig. 7, we compare the SE of the FD-assisted MTW-MMR systems with that of the corresponding HD-assisted MTW-MMR systems, in terms of the power of self-loop interference and inter-user interference, expressed as $\sigma^2 = \sigma_{RR}^2 = \sigma_{k,i}^2$. For $N = 500$, we observe that the FD mode outperforms the HD mode, provided that σ^2 is smaller than -15dB. In this case, the FD mode can efficiently exploit the time resources. However, when σ^2 becomes larger than -15dB, the SE of the HD mode is better than that of the FD mode, due to the severe self-loop interference and inter-user interference in the FD mode. Specifically, at $\sigma^2 = 0$, the loop interference channel is equally strong as the user channel, which significantly degrades the performance of the FD-assisted MTW-MMR system, resulting that the HD mode significantly outperforms the FD mode. In this case, more antennas are needed to resist the self-loop interference and the inter-user interference in the FD mode.

V. CONCLUSIONS

In this paper, we have investigated the SE and EE performance of the MTW-MMR systems by taking into account of both channel estimation error and channel aging effect. Assuming that all the nodes are operated in either FD or HD mode, we have derived the formulas for the SE and EE of the MTW-MMR systems employing MRC/MRT or ZFR/ZFT relay processing. In our analysis, we have addressed four types of power scaling schemes for different operational scenarios. Our studies and simulation results show that among the power-scaling schemes considered, the one in Case 3 is capable of achieving a good performance tradeoff between the SE and EE. For all the cases considered, channel aging results in reduction of both the achievable SE and the EE, as the result that channel estimation becomes less reliable when channels become less correlated. In both FD and HD modes, the inter-pair interference and self-interference can be effectively eliminated by the MRC/MRT or ZFR/ZFT relay processing. Furthermore, when the relay has a big number of antennas, when comparing the performance of the MTW-MMR systems in the FD mode with that in the HD mode, it is shown that the FD mode performs better than the HD mode, provided that σ^2 is smaller than -15dB. In practice, more antennas employed by the relay allows the FD-assisted MTW-MMR system to resist both the self-loop interference and the inter-user interference.

APPENDIX A
PROOF OF THEOREM 1

When the MRC/MRT relaying processing is employed by the FD-assisted MTW-MMR systems, $P_k(n)$ and $P_I(n)$ in (26) can be derived from (4) and be given as (69) and (70), as shown at the bottom of this page, respectively.

From formula (5), we have

$$N^{\frac{3}{2}}\tilde{\alpha}(n) = \sqrt{\frac{P_R}{P_S\cdot\frac{\tilde{\Delta}_1(n)}{N^3}+\frac{\sigma_{nr}^2}{N}\cdot\frac{\tilde{\Delta}_2(n)}{N^2}+\frac{\tilde{\Delta}_3(n)}{N^3}}}. \tag{71}$$

As $N\to\infty$, the terms in (71) can be simplified as (72)-(74) with the aid of (6)-(8).

$$\begin{aligned}
&\lim_{N\to\infty}\left[\frac{\tilde{\Delta}_1(n)}{N^3}\right] \\
&= \lim_{N\to\infty}\left[\mathrm{Tr}\left(\frac{\tilde{\boldsymbol{W}}_{mr}(0)\boldsymbol{H}_u(n-1)\boldsymbol{H}_u^H(n-1)\tilde{\boldsymbol{W}}_{mr}(0)^H}{N^3}\right)\right] \\
&= \lim_{N\to\infty}\left[\rho^{2(n-1)}\mathrm{Tr}\left(\left(\frac{\tilde{\boldsymbol{H}}_d^H(0)\tilde{\boldsymbol{H}}_d(0)}{N}\right)^T\boldsymbol{T}\right.\right. \\
&\quad\left.\left.\times\left(\frac{\tilde{\boldsymbol{H}}_u^H(0)\tilde{\boldsymbol{H}}_u(0)}{N}\right)^2\boldsymbol{T}\right)\right] \\
&\quad+\lim_{N\to\infty}\left[\frac{\rho^{2(n-1)}}{N}\mathrm{Tr}\left(\left(\frac{\tilde{\boldsymbol{H}}_d^H(0)\tilde{\boldsymbol{H}}_d(0)}{N}\right)^T\boldsymbol{T}\right.\right. \\
&\quad\left.\left.\times\left(\frac{\tilde{\boldsymbol{H}}_u^H(0)\boldsymbol{E}_u(n-1)}{\sqrt{N}}\right)^2\boldsymbol{T}\right)\right] \\
&= \rho^{2(n-1)}\sum_{i=1}^{2K}\hat{\sigma}_{di}^2\hat{\sigma}_{ui'}^4,
\end{aligned} \tag{72}$$

$$P_k(n) = \rho^{2(n-1)}\phi^{2n}P_S\mathbb{E}\left\|\tilde{\boldsymbol{h}}_{dk}^T(0)\tilde{\boldsymbol{W}}_{mr}(0)\tilde{\boldsymbol{h}}_{uk'}(0)\right\|^2, \tag{69}$$

$$\begin{aligned}
P_I(n) &= P_S\mathbb{E}\left\{\phi^{2n}\left\|\tilde{\boldsymbol{h}}_{dk}^T(0)\tilde{\boldsymbol{W}}_{mr}(0)\boldsymbol{e}_{uk'}(n-1)\right\|^2+\rho^{2(n-1)}\left\|\boldsymbol{e}_{dk}^T(n)\tilde{\boldsymbol{W}}_{mr}(0)\tilde{\boldsymbol{h}}_{uk'}(0)\right\|^2+\left\|\boldsymbol{e}_{dk}^T(n)\tilde{\boldsymbol{W}}_{mr}(0)\boldsymbol{e}_{uk'}(n-1)\right\|^2\right\} \\
&\quad+P_S\mathbb{E}\left\{\phi^{2n}\left\|\tilde{\boldsymbol{h}}_{dk}^T(0)\tilde{\boldsymbol{W}}_{mr}(0)\boldsymbol{e}_{uk}(n-1)\right\|^2+\rho^{2(n-1)}\left\|\boldsymbol{e}_{dk}^T(n)\tilde{\boldsymbol{W}}_{mr}(0)\tilde{\boldsymbol{h}}_{uk}(0)\right\|^2+\left\|\boldsymbol{e}_{dk}^T(n)\tilde{\boldsymbol{W}}_{mr}(0)\boldsymbol{e}_{uk}(n-1)\right\|^2\right\} \\
&\quad+P_S\mathbb{E}\left\{\phi^{2n}\rho^{2(n-1)}\left\|\tilde{\boldsymbol{h}}_{dk}^T(0)\tilde{\boldsymbol{W}}_{mr}(0)\sum_{\substack{j=1\\ j\neq k,k'}}^{2K}\tilde{\boldsymbol{h}}_{uj}(0)\right\|^2+\phi^{2n}\left\|\tilde{\boldsymbol{h}}_{dk}^T(0)\tilde{\boldsymbol{W}}_{mr}(0)\sum_{\substack{j=1\\ j\neq k,k'}}^{2K}\boldsymbol{e}_{uj}(n-1)\right\|^2\right. \\
&\quad\left.+\rho^{2(n-1)}\left\|\boldsymbol{e}_{dk}^T(n)\tilde{\boldsymbol{W}}_{mr}(0)\sum_{\substack{j=1\\ j\neq k,k'}}^{2K}\tilde{\boldsymbol{h}}_{uj}(0)\right\|^2+\left\|\boldsymbol{e}_{dk}^T(n)\tilde{\boldsymbol{W}}_{mr}(0)\sum_{\substack{j=1\\ j\neq k,k'}}^{2K}\boldsymbol{e}_{uj}(n-1)\right\|^2\right\} \\
&\quad+P_R\mathbb{E}\left\{\phi^{2n}\left\|\boldsymbol{h}_{dk}^T(0)\tilde{\boldsymbol{W}}_{mr}(0)\boldsymbol{H}_{RR}(n-1)\right\|^2\right\}+\sigma_{nr}^2\mathbb{E}\left\{\phi^{2n}\left\|\boldsymbol{h}_{dk}^T(0)\tilde{\boldsymbol{W}}_{mr}(0)\right\|^2\right\}+\frac{\sum_{i,k\in\mathcal{U}_k}\sigma_{k,i}^2P_S}{(\tilde{\alpha}(n))^2}+\frac{\sigma_n^2}{(\tilde{\alpha}(n))^2}.
\end{aligned} \tag{70}$$

$$\begin{aligned}
&\lim_{N\to\infty}\left[\frac{\tilde{\Delta}_2(n)}{N^2}\right] \\
&= \lim_{N\to\infty}\left[\frac{\mathrm{Tr}\left(\tilde{\boldsymbol{W}}_{mr}(0)\,\tilde{\boldsymbol{W}}_{mr}^H(0)\right)}{N^2}\right] \\
&= \lim_{N\to\infty}\left[\mathrm{Tr}\left(\left(\frac{\tilde{\boldsymbol{H}}_d^H(0)\tilde{\boldsymbol{H}}_d(0)}{N}\right)^T \boldsymbol{T}\left(\frac{\tilde{\boldsymbol{H}}_u^H(0)\tilde{\boldsymbol{H}}_u(0)}{N}\right)\boldsymbol{T}\right)\right] \\
&= \sum_{i=1}^{2K}\hat{\sigma}_{di}^2\hat{\sigma}_{ui'}^2,
\end{aligned} \tag{73}$$

$$\begin{aligned}
&\lim_{N\to\infty}\left[\frac{\tilde{\Delta}_3(n)}{N^3}\right] \\
&= \lim_{N\to\infty}\left[P_R\mathrm{Tr}\left(\frac{\tilde{\boldsymbol{W}}_{mr}(0)\,\boldsymbol{H}_{RR}\boldsymbol{H}_{RR}^H\tilde{\boldsymbol{W}}_{mr}(0)^H}{N^3}\right)\right] \\
&= \lim_{N\to\infty}\left[\frac{P_R}{N}\mathrm{Tr}\left(\boldsymbol{T}\left(\frac{\tilde{\boldsymbol{H}}_d^H(0)\tilde{\boldsymbol{H}}_d(0)}{N}\right)^T\boldsymbol{T}\right.\right. \\
&\quad \left.\left.\times\left(\frac{\tilde{\boldsymbol{H}}_u^H(0)\boldsymbol{H}_{RR}}{\sqrt{N}}\right)\left(\frac{\tilde{\boldsymbol{H}}_d^H(0)\boldsymbol{H}_{RR}}{\sqrt{N}}\right)^H\right)\right] \\
&= 0.
\end{aligned} \tag{74}$$

Therefore, we have

$$\lim_{N\to\infty}\frac{\sigma_{nr}^2}{N}\frac{\tilde{\Delta}_2(n)}{N^2}\to 0. \tag{75}$$

Therefore, by substituting (72), (74) and (75) into (71), we can obtain

$$\lim_{N\to\infty}\left(N^{\frac{3}{2}}\tilde{\alpha}(n)\right) = \sqrt{\frac{P_R}{P_S\cdot\rho^{2(n-1)}\sum_{i=1}^{2K}\hat{\sigma}_{di}^2\hat{\sigma}_{ui'}^4}}. \tag{76}$$

Therefore, when N tends to infinity, based on [50, Lemma 1], we can derive for the asymptotic signal power $P_k(n)$ and the interference plus noise power $P_I(n)$, which are given by (77) and (78), as shown at the bottom of this page.

In (78), the term $P_S a_{mr}$ is contributed by the channel estimation errors, the term $P_R b_{mr}$ is by the self-loop interference on the relay, while the term $\frac{\sigma_{nr}^2}{N}d_{mr}$ denotes the noise power on the relay. Furthermore, $\frac{\sum_{i,k\in U_k}\sigma_{k,i}^2 P_S}{\left(N^2\tilde{\alpha}(n)\right)^2}$ represents the self-loop interference and inter-user interference on user k, and finally, $\frac{\sigma_n^2}{\left(N^2\tilde{\alpha}(n)\right)^2}$ represents the noise power at user k.

Upon substituting $P_S = E_S$, $P_R = E_R$, (77) and (78) into (26) and (25), we can obtain (37). Furthermore, by substituting (37) into (27), we can obtain (38).

When all the involved nodes are operated in the HD mode, from (12), we can obtain

$$\lim_{N\to\infty}\left(N^{\frac{3}{2}}\tilde{\alpha}(n)\right) = \sqrt{\frac{P_R}{P_S\cdot\rho^{2(n-1)}\sum_{i=1}^{2K}\hat{\sigma}_{di}^2\hat{\sigma}_{ui'}^4}} \tag{79}$$

by following the similar analysis of (71).

Remembering that the power of the desired signal in the HD mode is the same as (77), when we compare it with

$$\lim_{N\to\infty}\left(\frac{P_k(n)}{N^4}\right) = \rho^{2(n-1)}\phi^{2n}P_S\left(\hat{\sigma}_{dk}^2\hat{\sigma}_{uk'}^2\right)^2, \tag{77}$$

$$\begin{aligned}
&\lim_{N\to\infty}\left(\frac{P_I(n)}{N^4}\right) \\
&= P_S\left\{\phi^{2n}\left(\hat{\sigma}_{dk}^4\hat{\sigma}_{uk'}^2\sigma_{e_{uk'}}^2(n-1)\right)+\rho^{2(n-1)}\left(\hat{\sigma}_{uk'}^4\hat{\sigma}_{dk}^2\sigma_{e_{dk}}^2(n)\right)+\hat{\sigma}_{dk}^2\hat{\sigma}_{uk'}^2\sigma_{e_{uk'}}^2(n-1)\,\sigma_{e_{dk}}^2(n)\right\} \\
&\quad + P_S\left\{\phi^{2n}\left(\hat{\sigma}_{dk}^4\hat{\sigma}_{uk'}^2\sigma_{e_{uk}}^2(n-1)\right)+\rho^{2(n-1)}\left(\hat{\sigma}_{uk'}^4\hat{\sigma}_{dk}^2\sigma_{e_{dk}}^2(n)\right)+\hat{\sigma}_{dk}^2\hat{\sigma}_{uk'}^2\sigma_{e_{uk}}^2(n-1)\,\sigma_{e_{dk}}^2(n)\right\} \\
&\quad + \underbrace{P_S\left\{\phi^{2n}\left(\hat{\sigma}_{dk}^4\hat{\sigma}_{uk'}^2\sum_{j\neq k,k'}^{2K}\sigma_{e_{uj}}^2(n-1)\right)+\rho^{2(n-1)}\left(\hat{\sigma}_{dk}^2\sigma_{e_{dk}}^2(n)\sum_{j\neq k,k'}^{2K}\hat{\sigma}_{uj}^4\right)+\hat{\sigma}_{dk}^2\hat{\sigma}_{uk'}^2\sum_{j\neq k,k'}^{2K}\left(\sigma_{e_{uj}}^2(n-1)\,\sigma_{e_{dj}}^2(n)\right)\right\}}_{=P_S a_{mr}} \\
&\quad + \underbrace{P_R\left\{\phi^{2n}\left(\hat{\sigma}_{dk}^4\hat{\sigma}_{uk'}^2\sigma_{RR}^2\right)+\sigma_{e_{dk}}^2(n)\,\hat{\sigma}_{dk}^2\hat{\sigma}_{uk'}^2\sigma_{RR}^2\right\}}_{=P_R b_{mr}} + \underbrace{\frac{\sigma_{nr}^2}{N}\left\{\phi^{2n}\left(\hat{\sigma}_{dk}^4\hat{\sigma}_{uk'}^2\right)+\sigma_{e_{dk}}^2(n)\,\hat{\sigma}_{dk}^2\hat{\sigma}_{uk'}^2\right\}}_{=\frac{\sigma_{nr}^2}{N}d_{mr}} + \frac{\sum_{i,k\in U_k}\sigma_{k,i}^2P_S}{\left(N^2\tilde{\alpha}(n)\right)^2} + \frac{\sigma_n^2}{\left(N^2\tilde{\alpha}(n)\right)^2}.
\end{aligned} \tag{78}$$

(78) in the FD mode, the $P_R b_{mr}$ term denoting the self-loop interference on the relay disappears in the HD mode, and the $\frac{\sum_{i,k\in U_k}\sigma_{k,i}^2 P_S}{(\tilde{\alpha}(n))^2}$ term of the self-loop interference on user k and inter-user interference also disappears in this case. Consequently, according to (28), we can obtain (39). Furthermore, from (39) we obtain the EE as shown in (40). This completes the proof of Theorem 1.

APPENDIX B
PROOF OF THEOREM 2

When the relay applies the ZFR/ZFT processing based on the aged CSI, (5) can be transformed into

$$\frac{\tilde{\alpha}(n)}{\sqrt{N}} = \sqrt{\frac{P_R}{P_S \cdot N\tilde{\Delta}_1(n) + \frac{\sigma_{nr}^2}{N}\cdot N^2\tilde{\Delta}_2(n) + N\tilde{\Delta}_3(n)}}. \tag{80}$$

When $N \to \infty$, we have

$$\begin{aligned}
&\lim_{N\to\infty}\left[N\tilde{\Delta}_1(n)\right]\\
&=\lim_{N\to\infty}\left[N\cdot\mathrm{Tr}\left(\tilde{\boldsymbol{W}}_{zf}(0)\boldsymbol{H}_u(n-1)\boldsymbol{H}_u^H(n-1)\tilde{\boldsymbol{W}}_{zf}(0)^H\right)\right]\\
&=\lim_{N\to\infty}\left[\frac{P_R}{N}\mathrm{Tr}\left(\left(\frac{\tilde{\boldsymbol{H}}_u^H(0)\tilde{\boldsymbol{H}}_u(0)}{N}\right)^{-1}\boldsymbol{T}\right.\right.\\
&\quad\times\left(\frac{\tilde{\boldsymbol{H}}_d^T(0)\tilde{\boldsymbol{H}}_d^*(0)}{N}\right)^{-1}\boldsymbol{T}\cdot\left(\frac{\tilde{\boldsymbol{H}}_u^H(0)\tilde{\boldsymbol{H}}_u(0)}{N}\right)^{-1}\\
&\quad\times\left.\left.\frac{\tilde{\boldsymbol{H}}_u^H(0)\boldsymbol{E}_u(n-1)}{\sqrt{N}}\left(\frac{\tilde{\boldsymbol{H}}_u^H(0)\boldsymbol{E}_u(n-1)}{\sqrt{N}}\right)^H\right)\right]\\
&\quad+\lim_{N\to\infty}\left[\rho^{2(n-1)}\mathrm{Tr}\left(\left(\frac{\tilde{\boldsymbol{H}}_d^T(0)\tilde{\boldsymbol{H}}_d^*(0)}{N}\right)^{-1}\right)\right]
\end{aligned}$$

$$=\rho^{2(n-1)}\sum_{i=1}^{2K}\frac{1}{\hat{\sigma}_{di}}, \tag{81}$$

$$\begin{aligned}
&\lim_{N\to\infty}\left[N^2\tilde{\Delta}_2(n)\right]\\
&=\lim_{N\to\infty}\left[N^2\cdot\mathrm{Tr}\left(\tilde{\boldsymbol{W}}_{zf}(0)\tilde{\boldsymbol{W}}_{zf}^H(0)\right)\right]\\
&=\lim_{N\to\infty}\left[\mathrm{Tr}\left(\left(\frac{\tilde{\boldsymbol{H}}_d^T(0)\tilde{\boldsymbol{H}}_d^*(0)}{N}\right)^{-1}\boldsymbol{T}\right.\right.\\
&\quad\times\left.\left.\left(\frac{\tilde{\boldsymbol{H}}_u^H(0)\tilde{\boldsymbol{H}}_u(0)}{N}\right)^{-1}\boldsymbol{T}\right)\right]
\end{aligned}$$

$$=\sum_{i=1}^{2K}\frac{1}{\hat{\sigma}_{di}^2\hat{\sigma}_{ui'}^2}, \tag{82}$$

$$\begin{aligned}
&\lim_{N\to\infty}\left[N\tilde{\Delta}_3(n)\right]\\
&=\lim_{N\to\infty}\left[N\cdot P_R\cdot\mathrm{Tr}\left(\tilde{\boldsymbol{W}}_{zf}(0)\boldsymbol{H}_{RR}\boldsymbol{H}_{RR}^H\tilde{\boldsymbol{W}}_{zf}^H(0)\right)\right]\\
&=\lim_{N\to\infty}\left[\frac{P_R}{N}\mathrm{Tr}\left(\left(\frac{\tilde{\boldsymbol{H}}_u^H(0)\tilde{\boldsymbol{H}}_u(0)}{N}\right)^{-1}\boldsymbol{T}\right.\right.\\
&\quad\times\left(\frac{\tilde{\boldsymbol{H}}_d^T(0)\tilde{\boldsymbol{H}}_d^*(0)}{N}\right)^{-1}\boldsymbol{T}\cdot\\
&\quad\left.\left.\left(\frac{\tilde{\boldsymbol{H}}_u^H(0)\tilde{\boldsymbol{H}}_u(0)}{N}\right)^{-1}\frac{\tilde{\boldsymbol{H}}_u^H(0)\boldsymbol{H}_{RR}}{\sqrt{N}}\left(\frac{\tilde{\boldsymbol{H}}_u^H(0)\boldsymbol{H}_{RR}}{\sqrt{N}}\right)^H\right)\right]
\end{aligned}$$

$$=0. \tag{83}$$

Therefore, when substituting (81)-(83) into (80), we can obtain

$$\lim_{N\to\infty}\left(\frac{\tilde{\alpha}(n)}{\sqrt{N}}\right)=\sqrt{\frac{P_R}{P_S\cdot\rho^{2(n-1)}\sum_{i=1}^{2K}\frac{1}{\hat{\sigma}_{di}^2}}}. \tag{84}$$

$$\lim_{N\to\infty}(P_k(n))=\rho^{2(n-1)}\phi^{2n}P_S, \tag{85}$$

$$\begin{aligned}
\lim_{N\to\infty}(P_I(n)) &= P_S\left\{\phi^{2n}\left(\frac{\sigma_{e_{uk'}}^2(n-1)}{\hat{\sigma}_{uk'}^2}\right)+\rho^{2(n-1)}\left(\frac{\sigma_{e_{dk}}^2(n)}{\hat{\sigma}_{dk}^2}\right)+\frac{\sigma_{e_{dk}}^2(n)\sigma_{e_{uk'}}^2(n-1)}{\hat{\sigma}_{dk}^2\hat{\sigma}_{uk'}^2}\right\}\\
&\quad\underbrace{\begin{aligned}&+P_S\left\{\phi^{2n}\left(\frac{\sigma_{e_{uk}}^2(n-1)}{\hat{\sigma}_{uk'}^2}\right)+\rho^{2(n-1)}\left(\frac{\sigma_{e_{dk}}^2(n)}{\hat{\sigma}_{dk}^2}\right)+\frac{\sigma_{e_{dk}}^2(n)\sigma_{e_{uk}}^2(n-1)}{\hat{\sigma}_{dk}^2\hat{\sigma}_{uk'}^2}\right\}\\&+P_S\left\{\phi^{2n}\left(\frac{\sum_{j\neq k,k'}^{2K}\sigma_{e_{uj}}^2(n-1)}{\hat{\sigma}_{uk'}^2}\right)+\rho^{2(n-1)}\left(\sigma_{e_{dk}}^2(n)\sum_{j\neq k,k'}^{2K}\frac{1}{\hat{\sigma}_{dj}^2}\right)+\frac{\sigma_{e_{dk}}^2(n)\sum_{j\neq k,k'}^{2K}\sigma_{e_{uj}}^2(n-1)}{\hat{\sigma}_{dk}^2\hat{\sigma}_{uk'}^2}\right\}\end{aligned}}_{=P_S a_{zf}}\\
&\quad+\underbrace{P_R\left(\phi^{2n}\left(\frac{\sigma_{RR}^2}{\hat{\sigma}_{uk'}^2}\right)+\frac{\sigma_{e_{dk}}^2(n)\sigma_{RR}^2}{\hat{\sigma}_{dk}^2\hat{\sigma}_{uk'}^2}\right)}_{=P_R b_{zf}}+\underbrace{\frac{\sigma_{nr}^2}{N}\left(\phi^{2n}\left(\frac{1}{\hat{\sigma}_{uk'}^2}\right)+\frac{\sigma_{e_{dk}}^2(n)}{\hat{\sigma}_{dk}^2\hat{\sigma}_{uk'}^2}\right)}_{=\frac{\sigma_{nr}^2}{N}d_{zf}}+\frac{\sum_{i,k\in\mathcal{U}_k}\sigma_{k,i}^2P_S}{(\tilde{\alpha}(n))^2}+\frac{\sigma_n^2}{(\tilde{\alpha}(n))^2}.
\end{aligned} \tag{86}$$

Furthermore, when $N \rightarrow \infty$, with the aid of [50, Lemma 1], we can derive the asymptotic $P_k(n)$ and $P_I(n)$, which are shown as (85) and (86), as shown at the bottom of the previous page.

In (86), $P_S a_{zf}$ is the combination of the channel estimation errors, $P_R b_{zf}$ is due to the self-loop interference on the relay, and $\frac{\sigma_{nr}^2}{N} d_{zf}$ is because of the noise added on the relay.

Finally, when we substitute $P_S = E_S$, $P_R = E_R$, (85) and (86) into (26), and then apply the result to (25) and (27), we can obtain (41) and (42). Similarly, when the MTW-MMR system is operated in HD mode and with the MRC/MRT processing, we can carry out the analysis to obtain (43) and (44) for the SE and EE.

APPENDIX C
PROOF OF THEOREM 3

In Case 3, by substituting $P_S = E_S$, $P_R = E_R/N$ into (77) and (78), and letting $N \rightarrow \infty$, we can obtain

$$\gamma_k^{FD}(n) = \frac{\rho^{2(n-1)}\phi^{2n}E_R\left(\hat{\sigma}_{dk}^2\hat{\sigma}_{uk'}^2\right)^2}{E_R a_{mr} + \rho^{2(n-1)}\sum_{i=1}^{2K}\hat{\sigma}_{di}^2\hat{\sigma}_{ui'}^4\left(\sum_{i,k\in U_k}\sigma_{k,i}^2 E_S + \sigma_n^2\right)}. \tag{87}$$

Then with the aid of (25), we can obtain (45). Finally, when substituting (45) into (27), we obtain(46) as $N \rightarrow \infty$.

In contrast to the FD mode, in the HD mode, both the self-loop interference and inter-user interference disappear. Thus, from (87) we can obtain the SINR in HD mode as

$$\gamma_k^{HD}(n) = \frac{\rho^{2(n-1)}\phi^{2n}E_R\left(\hat{\sigma}_{dk}^2\hat{\sigma}_{uk'}^2\right)^2}{E_R a_{mr} + \rho^{2(n-1)}\sum_{i=1}^{2K}\hat{\sigma}_{di}^2\hat{\sigma}_{ui'}^4\sigma_n^2}. \tag{88}$$

Consequently, by substituting (87) into (25) and (27), (88) into (27) and (28), respectively, we can obtain (45)-(48).

APPENDIX D
PROOF OF THEOREM 4

Theorem 4 can be proved following the same steps for Theorem 3, by taking of the ZFR/ZFT processing into account. In summary, the SINR in FD mode is

$$\gamma_k^{FD}(n) = \frac{\rho^{2(n-1)}\phi^{2n}E_R}{E_R a_{zf} + \rho^{2(n-1)}\sum_{i=1}^{2K}\frac{1}{\hat{\sigma}_{di}}\left(\sum_{i,k\in U_k}\sigma_{k,i}^2 E_S + \sigma_n^2\right)}, \tag{89}$$

and that in HD mode is

$$\gamma_k^{HD}(n) = \frac{\rho^{2(n-1)}\phi^{2n}E_R}{E_R a_{zf} + \rho^{2(n-1)}\sum_{i=1}^{2K}\frac{1}{\hat{\sigma}_{di}}\sigma_n^2}. \tag{90}$$

Consequently, with the aid of (25), (27), and (28), we can obtain (49)-(52).

APPENDIX E
PROOF OF THEOREM 5

For Theorem 5 in the Case 3 with $P_S = E_S/N$, $P_R = E_R/N$, we can derive to obtain

$$\gamma_k^{FD}(n) = \frac{\rho^{2(n-1)}\phi^{2n}E_R E_S\left(\hat{\sigma}_{dk}^2\hat{\sigma}_{uk'}^2\right)^2}{E_R E_S a_{mr} + E_R^2 b_{mr} + \sigma_{nr}^2 E_R d_{mr} + E_S\sigma_n^2\rho^{2(n-1)}\sum_{i=1}^{2K}\hat{\sigma}_{di}^2\hat{\sigma}_{ui'}^4}, \tag{91}$$

in the FD mode. By contrast, in the HD mode, it can be shown that the SINR is

$$\gamma_k^{HD}(n) = \frac{\rho^{2(n-1)}\phi^{2n}E_R E_S\left(\hat{\sigma}_{dk}^2\hat{\sigma}_{uk'}^2\right)^2}{E_R E_S a_{mr} + \sigma_{nr}^2 E_R d_{mr} + E_S\sigma_n^2\rho^{2(n-1)}\sum_{i=1}^{2K}\hat{\sigma}_{di}^2\hat{\sigma}_{ui'}^4}. \tag{92}$$

Consequently, (53)-(56) can be obtained by substituting (91) into (25) and (27), (92) into (27) and (28), respectively in the FD and HD modes.

APPENDIX F
PROOF OF THEOREM 6

When the ZFR/ZFT relay processing is operated in Case 3, in the FD mode, we have

$$\gamma_k^{FD}(n) = \frac{\rho^{2(n-1)}\phi^{2n}E_S E_R}{E_S E_R a_{zf} + E_R^2 b_{zf} + \sigma_{nr}^2 E_R d_{zf} + E_S\sigma_n^2\rho^{2(n-1)}\sum_{i=1}^{2K}\frac{1}{\hat{\sigma}_{di}}}, \tag{93}$$

and in the HD mode, we have

$$\gamma_k^{HD}(n) = \frac{\rho^{2(n-1)}\phi^{2n}E_S E_R}{E_S E_R a_{zf} + \sigma_{nr}^2 E_R d_{zf} + E_S\sigma_n^2\rho^{2(n-1)}\sum_{i=1}^{2K}\frac{1}{\hat{\sigma}_{di}}}, \tag{94}$$

applying (93) and (94) respectively to (25) and (28), and according to (27), we obtain (57)-(60).

APPENDIX G
PROOF OF THEOREM 7

In Case 4, if $P_S = E_S/N$ and $P_R = E_R$, it can be shown from (77)-(78) that

$$\gamma_k^{FD}(n) = 0. \tag{95}$$

Consequently, the SE and EE of the MTW-MMR system employing the MRC/MRT processing and operated in the FD mode tend to 0, as $N \rightarrow \infty$.

By contrast, when in the HD mode, we can obtain

$$\gamma_k^{HD}(n) = \frac{\rho^{2(n-1)}\phi^{2n}E_S\left(\hat{\sigma}_{dk}^2\hat{\sigma}_{uk'}^2\right)^2}{E_S a_{mr} + \sigma_{nr}^2 d_{mr}}. \tag{96}$$

Consequently, we can obtain get (63)-(64) by substituting (96) into (27) and (28).

APPENDIX H
PROOF OF THEOREM 8

Similarly, when the ZFR/ZFT relay processing is employed, we have

$$\gamma_k^{FD}(n) = 0. \tag{97}$$

Here, the SE and EE of the FD-assisted MTW-MMR system employing the ZFR/ZFT processing also tend to 0 as $N \to \infty$.

By contrast, when operated in the HD mode, we have

$$\gamma_k^{HD}(n) = \frac{\rho^{2(n-1)}\phi^{2n}E_S}{E_S a_{zf} + \sigma_{nr}^2 d_{zf}}. \tag{98}$$

Substituting it to (27) and (28), respectively, we obtain (67)-(68).

ACKNOWLEDGMENT

This paper was presented in part at the 2017 IEEE GLOBECOM [1].

REFERENCES

[1] J. He, L. Li, H. Zhang, W. Chen, L. Yang, and Z. Han, "Multi-pair bidirectional relaying with full-duplex massive MIMO experiencing channel aging," in *Proc. IEEE GLOBECOM*, Singapore, Dec. 2017, pp. 1–6.
[2] J. G. Andrews *et al.*, "What will 5G be?" *IEEE J. Sel. Areas Commun.*, vol. 32, no. 6, pp. 1065–1082, Jun. 2014.
[3] J. Shi, L. Lv, Q. Ni, H. Pervaiz, and C. Paoloni, "Modeling and analysis of point-to-multipoint millimeter wave backhaul networks," *IEEE Trans. Wireless Commun.*, vol. 18, no. 1, pp. 268–285, Jan. 2019.
[4] S. Han, S. Xu, W. Meng, and C. Li, "Dense-device-enabled cooperative networks for efficient and secure transmission," *IEEE Netw.*, vol. 32, no. 2, pp. 100–106, Mar./Apr. 2018.
[5] E. G. Larsson, O. Edfors, F. Tufvesson, and T. L. Marzetta, "Massive MIMO for next generation wireless systems," *IEEE Commun. Mag.*, vol. 52, no. 2, pp. 186–195, Feb. 2014.
[6] P. Murphy and A. Sabharwal, "Design, implementation, and characterization of a cooperative communications system," *IEEE Trans. Veh. Technol.*, vol. 60, no. 6, pp. 2534–2544, Jul. 2011.
[7] Y. Liao, L. Song, Z. Han, and Y. Li, "Full duplex cognitive radio: A new design paradigm for enhancing spectrum usage," *IEEE Commun. Mag.*, vol. 53, no. 5, pp. 138–145, May 2015.
[8] L. Song, Y. Li, and Z. Han, "Resource allocation in full-duplex communications for future wireless networks," *IEEE Wireless Commun.*, vol. 22, no. 4, pp. 88–96, Aug. 2015.
[9] L. Song, R. Wichman, Y. Li, and Z. Han, *Full-Duplex Communications and Networks*. Cambridge, U.K.: Cambridge Univ. Press, 2017.
[10] J. Fan, L. Li, T. Bao, and H. Zhang, "Two-way relaying with differential MPSK modulation in virtual full duplexing system," in *Proc. IEEE Int. Conf. Signal Process., Commun. Comput. (ICSPCC)*, Ningbo, China, Sep. 2015, pp. 1–5.
[11] H. A. Suraweera, H. Q. Ngo, T. Q. Duong, C. Yuen, and E. G. Larsson, "Multi-pair amplify-and-forward relaying with very large antenna arrays," in *Proc. IEEE Int. Conf. Commun. (ICC)*, Budapest, Hungary, Jun. 2013, pp. 4635–4640.
[12] J. Fan, L. Li, and H. Zhang, "Full-duplex denoise-and-forward two-way relaying with DBPSK modulation," in *Proc. Int. Conf. Wireless Commun. Signal Process. (WCSP)*, Yangzhou, China, Oct. 2016, pp. 1–5.
[13] J. Fan, L. Li, H. Zhang, and W. Chen, "Denoise-and-forward two-path successive relaying with DBPSK modulation," *IEEE Wireless Commun. Lett.*, vol. 6, no. 1, pp. 42–45, Feb. 2017.
[14] S. Han, Y. Zhang, W. Meng, and H.-H. Chen, "Self-interference-cancelation-based SLNR precoding design for full-duplex relay-assisted system," *IEEE Trans. Veh. Technol.*, vol. 67, no. 9, pp. 8249–8262, Sep. 2018.
[15] L. Li, Y. Xu, Z. Zhang, J. Yin, W. Chen, and Z. Han, "A prediction-based charging policy and interference mitigation approach in the wireless powered Internet of Things," *IEEE J. Sel. Areas Commun.*, vol. 37, no. 2, pp. 439–451, Feb. 2019.
[16] H. Q. Ngo, H. A. Suraweerat, M. Matthaiou, and E. G. Larsson, "Multipair massive MIMO full-duplex relaying with MRC/MRT processing," in *Proc. IEEE Int. Conf. Commun. (ICC)*, Sydney, NSW, Australia, Jun. 2014, pp. 4807–4813.
[17] Z. Zhang, Z. Chen, M. Shen, B. Xia, and L. Luo, "Achievable rate analysis for multi-pair two-way massive MIMO full-duplex relay systems," in *Proc. IEEE Int. Symp. Inf. Theory (ISIT)*, Hong Kong, Jun. 2015, pp. 2598–2602.
[18] Z. Zhang, Z. Chen, M. Shen, and B. Xia, "On capacity of two-way massive MIMO full-duplex relay systems," in *Proc. IEEE Int. Conf. Commun. (ICC)*, London, U.K., Jun. 2015, pp. 4327–4332.
[19] J. Yang, H. Wang, J. Ding, B. Li, and C. Li, "Spectral and energy efficiency for massive MIMO multi-pair two-way relay networks with ZFR/ZFT and imperfect CSI," in *Proc. IEEE Asia–Pacific Conf. Commun.*, Kyoto, Japan, Oct. 2015, pp. 47–51.
[20] Z. Zhang, Z. Chen, H. Feng, M. Shen, B. Xia, and L. Luo, "Statistical rate analysis for multi-pair two-way full-duplex relaying with massive antennas," in *Proc. IEEE Wireless Commun. Netw. Conf. (WCNC)*, Doha, Qatar, Apr. 2016, pp. 1–7.
[21] J. Feng, S. Ma, G. Yang, and H. V. Poor, "Impact of antenna correlation on full-duplex two-way massive MIMO relaying systems," *IEEE Trans. Wireless Commun.*, vol. 17, no. 6, pp. 3572–3587, Jun. 2018.
[22] J. Yang, H. Wang, J. Ding, X. Gao, and Z. Ding, "Spectral and energy efficiency analysis for massive MIMO multi-pair two-way relaying networks under generalized power scaling," *Sci. China Inf. Sci.*, vol. 60, no. 10, pp. 102303:1–102303:14, Mar. 2017.
[23] Z. Zhang, Z. Chen, M. Shen, and B. Xia, "Spectral and energy efficiency of multipair two-way full-duplex relay systems with massive MIMO," *IEEE J. Sel. Areas Commun.*, vol. 34, no. 4, pp. 848–863, Apr. 2016.
[24] S. Jin, X. Liang, K.-K. Wong, X. Gao, and Q. Zhu, "Ergodic rate analysis for multipair massive MIMO two-way relay networks," *IEEE Trans. Wireless Commun.*, vol. 14, no. 3, pp. 1480–1491, Mar. 2015.
[25] H. Wang, J. Ding, J. Yang, X. Gao, and Z. Ding, "Spectral and energy efficiency for multi-pair massive MIMO two-way relaying networks with imperfect CSI," in *Proc. IEEE Veh. Technol. Conf. (VTC Fall)*, Boston, MA, USA, Sep. 2015, pp. 1–6.
[26] C. Kong, C. Zhong, M. Matthaiou, E. Björnson, and Z. Zhang, "Multi-pair two-way AF relaying systems with massive arrays and imperfect CSI," in *Proc. IEEE Int. Conf. Acoust., Speech Signal Process. (ICASSP)*, Shanghai, China, Mar. 2016, pp. 3651–3655.
[27] S. Silva, G. Amarasuriya, C. Tellambura, and M. Ardakani, "Massive MIMO two-way relay networks with channel imperfections," in *Proc. IEEE Int. Conf. Commun. (ICC)*, Kuala Lumpur, Malaysia, May 2016, pp. 1–7.
[28] Z. Fang, W. Ni, F. Liang, P. Shao, and Y. Wu, "Massive MIMO for full-duplex cellular two-way relay network: A spectral efficiency study," *IEEE Access*, vol. 5, pp. 23288–23298, 2017.
[29] J. Feng, S. Ma, G. Yang, and B. Xia, "Power scaling of full-duplex two-way massive MIMO relay systems with correlated antennas and MRC/MRT processing," *IEEE Trans. Wireless Commun.*, vol. 16, no. 7, pp. 4738–4753, Jul. 2017.
[30] C. Xu, J. Yang, L. Zhou, and Y. Du, "Achievable rate analysis for multi-pair two-way amplify-and-forward MIMO system in Ricean fading," in *Proc. IEEE Int. Conf. Ubiquitous Future Netw. (ICUFN)*, Vienna, Austria, Jul. 2016, pp. 313–318.
[31] X. Wang, Y. Wang, and R. Sun, "Approximate sum rate for massive multiple-input multiple-output two-way relay with Ricean fading," *IET Commun.*, vol. 10, no. 12, pp. 1493–1500, 2016.
[32] X. Sun, K. Xu, W. Ma, Y. Xu, X. Xia, and D. Zhang, "Multi-pair two-way massive MIMO AF full-duplex relaying with imperfect CSI over Ricean fading channels," *IEEE Access*, vol. 4, pp. 4933–4945, 2016.
[33] X. Sun, K. Xu, W. Xie, X. Han, and Y. Xu, "Multi-pair two-way massive MIMO AF relaying with MRC/MRT and imperfect CSI," in *Proc. IEEE/CIC Int. Conf. Commun. China (ICCC)*, Chengdu, China, Jul. 2016, pp. 1–6.
[34] X. Sun, K. Xu, W. Ma, and Y. Xu, "Multi-pair two-way massive MIMO AF full-duplex relaying with ZFR/ZFT and imperfect CSI," *IEEE Int. Symp. Commun.and Inf.Technologies (ISCIT)*, Qingdao, China, Sep. 2016, pp. 27–32.

[35] K. P. Roshandeh, A. Kuhestani, M. Ardakani, and C. Tellambura, ''Ergodic sum rate analysis and efficient power allocation for a massive MIMO two-way relay network,'' *IET Commun.*, vol. 11, no. 2, pp. 211–217, Jan. 2017.

[36] P. Xing, J. Liu, C. Zhai, X. Wang, and X. Zhang, ''Multipair two-way full-duplex relaying with massive array and power allocation,'' *IEEE Trans. Veh. Technol.*, vol. 66, no. 10, pp. 8926–8939, Oct. 2017.

[37] Z. Zhang, Z. Chen, M. Shen, B. Xia, W. Xie, and Y. Zhao, ''Performance analysis for training-based multipair two-way full-duplex relaying with massive antennas,'' *IEEE Trans. Veh. Technol.*, vol. 66, no. 7, pp. 6130–6145, Jul. 2017.

[38] X. Pan, L. Guo, C. Dong, and T. Kang, ''Secure multi-pair massive MIMO two-way amplify-and-forward relay network with power allocation scheme,'' in *Proc. IEEE Int. Conf. Commun. (ICC)*, Paris, France, May 2017, pp. 1–5.

[39] K. T. Truong and R. W. Heath, Jr., ''Effects of channel aging in massive MIMO systems,'' *J. Commun. Netw.*, vol. 15, no. 4, pp. 338–351, 2013.

[40] C. Kong, C. Zhong, A. K. Papazafeiropoulos, and M. Matthaiou, ''Effect of channel aging on the sum rate of uplink massive MIMO systems,'' in *Proc. IEEE Int. Symp. Inf. Theory (ISIT)*, Jun. 2015, vol. 7, no. 4, pp. 1222–1226.

[41] Q. Bao, H. Wang, Y. Chen, and C. Liu, ''Downlink sum-rate and energy efficiency of massive MIMO systems with channel aging,'' in *Proc. Int. Conf. Wireless Commun. Signal Process. (WCSP)*, Yangzhou, China, Oct. 2016, pp. 1–5.

[42] A. K. Papazafeiropoulos, ''Impact of general channel aging conditions on the downlink performance of massive MIMO,'' *IEEE Trans. Veh. Technol.*, vol. 66, no. 2, pp. 1428–1442, Feb. 2017.

[43] A. K. Papazafeiropoulos, ''Downlink performance of massive MIMO under general channel aging conditions,'' in *Proc. IEEE GLOBECOM*, San Diego, CA, USA, Dec. 2015, pp. 1–6.

[44] C. Kong, C. Zhong, A. K. Papazafeiropoulos, M. Matthaiou, and Z. Zhang, ''Sum-rate and power scaling of massive MIMO systems with channel aging,'' in *Proc. IEEE GLOBECOM*, San Diego, CA, USA, Dec. 2015, pp. 4879–4893.

[45] J. Li, D. Wang, P. Zhu, and X. You, ''Uplink spectral efficiency analysis of distributed massive MIMO with channel impairments,'' *IEEE Access*, vol. 5, pp. 5020–5030, 2017.

[46] Y. Chen, C. Liu, H. Wang, and W.-P. Zhu, ''Effect of composite channel aging on the spectral efficiency of multi-pair massive multiple-input multiple-output amplify-and-forward relay networks,'' *IET Commun.*, vol. 11, no. 8, pp. 1313–1324, Jun. 2017.

[47] J. Feng, Z. Shi, and S. Ma, ''Sum rate of full-duplex two-way massive MIMO relay systems with channel aging,'' in *Proc. ICCS*, Shenzhen, China, Dec. 2016, pp. 1–6.

[48] G. Liu, F. G. Yu, H. Ji, V. C. M. Leung, and X. Li, ''In-band full-duplex relaying: A survey, research issues and challenges,'' *IEEE Commun. Surveys Tuts.*, vol. 17, no. 2, pp. 500–524, 2nd Quart., 2015.

[49] H. Q. Ngo, E. G. Larsson, and T. L. Marzetta, ''Energy and spectral efficiency of very large multiuser MIMO systems,'' *IEEE Trans. Commun.*, vol. 61, no. 4, pp. 1436–1449, Apr. 2013.

[50] H. Cui, L. Song, and B. Jiao, ''Multi-pair two-way amplify-and-forward relaying with very large number of relay antennas,'' *IEEE Trans. Wireless Commun.*, vol. 13, no. 5, pp. 2636–2645, May 2014.

LIXIN LI (M'12) received the B.Sc. and M.Sc. degrees in communication engineering and the Ph.D. degree in control theory and its applications from Northwestern Polytechnical University (NPU), Xi'an, China, in 2001, 2004, and 2008, respectively. He was a Postdoctoral Fellow with NPU, from 2008 to 2010. In 2017, he was a Visiting Scholar with the University of Houston, TX, USA. He is currently an Associate Professor with the School of Electronics and Information, NPU. He has authored or coauthored over 80 technical papers in journals and international conferences. He holds ten patents. His current research interests include wireless communications, game theory, and machine learning. He received the 2016 NPU Outstanding Young Teacher Award, which is the highest research and education honors for young faculties in NPU. He has reviewed papers for many international journals.

JIAO HE received the B.Sc. degree in communication engineering and the M.Sc. degree in communication and information systems from Northwestern Polytechnical University, Xi'an, China, in 2015 and 2018, respectively. She is currently a Technical Personnel of the Xi'an ASN Technology Group Co., Ltd. Her research interests include massive multiple input multiple output (MIMO), cooperative relaying, and full-duplex technology.

LIE-LIANG YANG (M'98–SM'02–F'16) received the B.Eng. degree in communications engineering from Shanghai Tiedao University, Shanghai, China, in 1988, and the M.Eng. and Ph.D. degrees in communications and electronics from Northern (Beijing) Jiaotong University, Beijing, China, in 1991 and 1997, respectively. In 1997, he was a Visiting Scientist with the Institute of Radio Engineering and Electronics, Academy of Sciences of the Czech Republic. Since 1997, he has been with The University of Southampton, U.K., where he is currently a Professor of wireless communications with the School of Electronics and Computer Science. He has published 350+ research papers in journals and conference proceedings, has authored or coauthored three books, and also published several book chapters. His research interests include wireless communications, wireless networks and signal processing for wireless communications, and molecular communications and nano-networks. The details about his research publications can be found at http://www.mobile.ecs.soton.ac.uk/lly/. He is a Distinguished Lecturer of the IEEE Vehicular Technology Society. He is a Fellow of the IET (previously IEE), U.K. He has served as an Associate Editor for several academic journals, has co-organized several special issues, and has acted in different roles for conference organization.

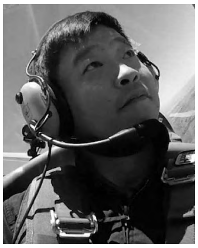

ZHU HAN (S'01–M'04–SM'09–F'14) received the B.S. degree in electronic engineering from Tsinghua University, in 1997, and the M.S. and Ph.D. degrees in electrical and computer engineering from the University of Maryland, College Park, in 1999 and 2003, respectively.

From 2000 to 2002, he was a Research and Development Engineer of JDSU, Germantown, MD, USA. From 2003 to 2006, he was a Research Associate with the University of Maryland. From 2006 to 2008, he was an Assistant Professor with Boise State University, ID, USA. He is currently a Professor with the Electrical and Computer Engineering Department, University of Houston, TX, USA, and also with the Computer Science Department, University of Houston. His research interests include wireless resource allocation and management, wireless communications and networking, game theory, big data analysis, security, and smart grid. He is currently an IEEE Communications Society Distinguished Lecturer. He was a recipient of the NSF Career Award, in 2010. He received the Fred W. Ellersick Prize from the IEEE Communication Society, in 2011, the EURASIP Best Paper Award for the *Journal on Advances in Signal Processing*, in 2015, the IEEE Leonard G. Abraham Prize in the field of Communications Systems (Best Paper Award in IEEE JSAC), in 2016, and several best paper awards from IEEE conferences.

MIAO PAN (S'07–M'12–SM'18) received the B.Sc. degree in electrical engineering from the Dalian University of Technology, China, in 2004, the M.A.Sc. degree in electrical and computer engineering from the Beijing University of Posts and Telecommunications, China, in 2007, and the Ph.D. degree in electrical and computer engineering from the University of Florida, in 2012. He is currently an Assistant Professor with the Department of Electrical and Computer Engineering, University of Houston. His research interests include big data privacy, cybersecurity, cyber-physical systems, and cognitive radio networking. He is a member of ACM. He was a recipient of the NSF CAREER Award, in 2014. His work received best paper awards from the VTC 2018, the Globecom 2017, and the Globecom 2015, respectively. He is an Associate Editor of the IEEE INTERNET OF THINGS (IoT) JOURNAL, from 2015 to 2018.

WEI CHEN (S'05–M'07–SM'13) received the B.S. and Ph.D. degrees (Hons.) from Tsinghua University, in 2002 and 2007, respectively.

From 2005 to 2007, he was a Visiting Ph.D. Student with The Hong Kong University of Science and Technology. From 2014 to 2016, he was the Deputy Head of the Department of Electronic Engineering. He visited Princeton University, Telecom ParisTech, and The University of Southampton, in 2016, 2014, and 2010, respectively. Since 2007, he has been a Faculty Member with Tsinghua University, where he is currently a Tenured Full Professor, the Director of Degree Office, and a University Council Member. His research interests include the areas of communication theory, stochastic optimization, and statistical learning. He is a Cheung Kong Young Scholar and a member of the National Program for Special Support for Eminent Professionals, also known as 10 000-Talent Program. He was a recipient of the IEEE Marconi Prize Paper Award, in 2009, and the IEEE Comsoc Asia Pacific Board Best Young Researcher Award, in 2011. He was also a recipient of the National May 1st Labor Medal and the China Youth May 4th Medal. He serves as an Editor for the IEEE TRANSACTIONS ON COMMUNICATIONS. He has been supported by the National 973 Youth Project, the NSFC Excellent Young Investigator Project, the New Century Talent Program of the Ministry of Education, and the Beijing Nova Program. He has served as a TPC Co-Chair for the IEEE VTC-Spring, in 2011, and as a Symposium Co-Chair for the IEEE ICC and Globecom.

HUISHENG ZHANG received the B.Sc. degree and the M.Sc. degree in electronic engineering from Northwestern Polytechnical University (NPU), Xi'an, China, in 1977 and 1986, respectively, where he is currently a Full Professor with the School of Electronics and Information. He has published more than 100 technical papers in refereed journals and conference proceedings. His current research interests include mobile communication and anti-jamming technology. He is a member of the Teaching Steering Committee of the Ministry of Education of the People's Republic of China. He was a recipient of the Distinguished Teacher Award of Shaanxi Province, in 2006.

XU LI received the B.Sc. degree in electronics and information technology, the M.Sc. degree in signal and information processing, and the Ph.D. degree in circuits and systems from Northwestern Polytechnical University, Xi'an, China, in 2001, 2004, and 2010, respectively. In 2004, he joined the School of Electronics and Information, Northwestern Polytechnical University. From 2007 to 2008, he was a Visiting Ph.D. Student with Telecom ParisTech (ENST), Paris, France. From 2012 to 2014, he was an Enterprise Postdoctoral Fellow with the Jiangsu Research and Development Center for Internet of Things, Wuxi, China. From 2015 to 2016, he was a Marie Currie Research Fellow with the School of Computer Science, University of Lincoln, Lincoln, U.K. He is currently an Associate Professor with the School of Electronics and Information, Northwestern Polytechnical University. His research interests include image fusion, image enhancement, and image super-resolution.